Title
Postnatal development of the bony orbit

Author
Lee, Yen-Ping,

Publication Date
1997

Peer reviewed|Thesis/dissertation

POSTNATAL DEVELOPMENT OF THE BONY ORBIT: A STUDY ON PA CEPHALOGRAMS

by

YEN-PING LEE, DDS

THESIS

Submitted in partial satisfaction of the requirements for the degree of

MASTER OF SCIENCE

in

ORAL BIOLOGY

in the

GRADUATE DIVISION

of the

UNIVERSITY OF CALIFORNIA

San Francisco

[redacted]

Date . . . . University Librarian

Degree Conferred: . . . .

ACKNOWLEDGEMENT

I would like to express my deepest gratitude to Dr. Karin Vargervik for being my mentor and for all her guidance and constant support not only in this project, but also in my residency. This thesis would not have been possible without all her efforts and patient instruction. Her dedication to the Orthodontic program is also appreciated.

I would also like to express my sincere gratitude to Dr. Sheldon Baumrind for being my mentor and allowing me to use his records. His guidance in research and generous help have brought this project to completion. His enthusiastic and rigorous attitude toward scientific research will always be an example in my life.

I would like to thank Dr. Sally Marshall, my committee member and my advisor for her review and support of my thesis. I also appreciate her dedication in improving the journal club for oral biology Masters Program.

I would like to thank Dr. Sean Carlson for all his invaluable assistance toward the completion of this project. I also wish to thank Dr. Jae-hyun Ahn and Dr. Ross Miller for all their technical support.

I also would like to thank for the financial support of this project from the UCSF Division of Orthodontics Fund for Excellence.

Last and most of all, I would like to express my appreciation to my family, my husband Ming-Guang and my mother. It is their enduring support and encouragement for the past years to help me complete the program. I dedicated this work to them and my son, Justin.

TABLE OF CONTENTS

LIST OF TABLES

LIST OF FIGURES

I. INTRODUCTION

Successful reconstructive surgery for craniofacial anomalies patients requires accurate diagnosis and careful planning. Outcome of surgical correction of craniofacial deformities are more predictive when accurate quantitative references and norms are available for planning. Surgical teams have been seeking quantitative data in order to better assess malformed craniofacial structures. An area which is always malformed and underdeveloped in individuals with one of the several craniosynostosis syndromes is the bony orbit. Accurate information about magnitude and timing of sagittal, vertical and transverse growth of the bony orbit is prerequisite for determining degree of malformation or underdevelopment of the orbit in individuals with a craniosynostosis syndrome or hypertelorism. Understanding the general normal growth pattern of the orbital complex will facilitate decisions concerning timing of intervention, effect of surgical intervention on skeletal growth, and proper positioning of the orbit relative to the globe and the rest of the midface. Norms for incremental growth of the orbital cavity in normal children can also improve our understanding of abnormal development.

This study reports longitudinal cephalometric data on the displacement and size and shape changes of the orbital cavity and its relationship to the anterior cranial base in a sample of twenty normal children with implant markers of the Björk type. P-A (posteroanterior) frontal images were used for this study. It is expected that the quantitative growth curves of the bony orbit generated in this study can be used as reference for planning reconstructive surgical procedures involving the orbit such as is the case in individuals with craniosynostosis or hypertelorism.

II. BACKGROUND

A. RECONSTRUCTIVE PROCEDURES INVOLVING THE ORBITS

Midface advancement by Le Fort III osteotomy developed by Tessier in the late 1960s and 1970s has been a common procedure in craniofacial reconstructive surgery in patients with craniosynostosis (Hogman and Willmar, 1974; Munro, 1978; Bu et al., 1989). Le Fort III surgery traditionally has been done in adolescents with most of their growth completed. Recently, in some centers, the procedure has been carried out at much earlier ages (before 5 years) to improve functional and psychological aspects (Waitzman et al, 1992). However, uncertainty exists as to the optimal timing for this major surgical intervention in growing patients . On one hand, one would wish to correct gross morphological disparities as early as possible, while on the other hand it is desirable to avoid interference with residual growth that may result from too early intervention and to avoid additional major surgical interventions later. One factor complicating the identification of the optimal time for surgical intervention has been the lack of information on the growth and displacement of the orbit in normal individuals.

B. GROWTH OF THE ORBITAL CAVITY

1. SAGITTAL GROWTH

There have been several implant studies on growth of the maxilla in children, but no specific information on orbital growth has been included in these studies. Iseri and Solow (1990) in a study of 14 girls with Bojrk implants, found that the sagittal maxillary sutural growth peaked at 11 and terminated at 18 years. The overall forward growth was about 5 mm from 6 to 20 years of age. Vertical growth peaked at 12 and terminated at 15 years with overall downward growth of 4.5 mm. The orbital cavity, as a connection between the neurocranium and maxilla, is expected to grow somewhat differently from the maxilla to serve as a bridge between the early neurocranial development and the later viscerocranial development.

In our previous study with the specific aim to assess forward displacement of the orbit in normal children, lateral cephalograms obtained yearly from 8.5 to 15.5 years of 36 subjects with Björk type implants were used (Lee et al.). The best landmark available on the lateral cephalogram for characterizing the antero-posterior position of the orbit is orbitale, defined as the inferiormost point on the image of the more anterior orbit. When utilizing anterior cranial base superimposition, the orbitale moved in the same direction as maxillary landmarks such as A and ANS (anterior nasal spine) points but at a slower rate. The mean forward displacement of orbitale from 8.8 years to 15.5 years of age was 1.5 mm, SD (standard deviation) =1.7 mm. The mean downward displacement was 1.8 mm, SD=1.3 mm.

Relative to the superimposition on the maxillary implants, orbitale demonstrated mean backward displacement of 2.1 mm, SD=1.7 mm, and upward displacement of 2.7 mm, SD=1.8 mm. Orbitale appeared to remodel in a direction opposite to that of maxillary sutural growth, showing a progressive superior deposition and posterior resorption. These observations appeared consistent with the finding of Waitzman et al. (1992) that the growth of the orbital cavity is closely related to neurocranial growth, which levels off in early childhood. It is also in accordance with Enlow's findings (1966). He stated that the floor of the orbit is lowered as a result of the increasing height of the frontal process of the maxilla during sutural growth. Corresponding surface deposition of new bone serves proportionately to relocate the orbital floor in a progressively superior direction. Sagittaly, simultaneously with maxillary forward growth as result of sutural growth, there is compensatory posterior resorption of the orbit, thereby constantly maintaining its position relative to the rest of the face.

2. TRANSVERSE GROWTH

In early stages of embryological development the optic placode and later the eye are positioned laterally, then converge forward and medially from their lateral primitive position to the frontal aspect of the face. Most of the convergence occurs before a definitive bony orbit is present. Any aberration in this development will arrest convergence during the prenatal period and leave the orbits in a primitive position on the side of the face (Costaras and Pruzansky, 1982).

Postnatal transverse growth of the orbit involves several mechanisms. The interorbital region occupies the mid-line between the neurocranium and facial skeleton. This region consists of the paranasal air sinuses. Frontal, nasal, maxillary, ethmoidal and sphenoid bones contribute to its morphology and growth (Morin et al.,1963). The process of growth includes:

1. Growth of surrounding structures

The neurocranium enlarges three times between birth and maturity. Waitzman et al. (1992) in a study using 542 CT scans, found that the cranial vault grows rapidly in the first year of life but growth levels off early. The expansion of the cranial vault follows the neural growth pattern and mainly affects the superior portion of the interorbital region.

2. Growth at the sutures:

There are several sutures involved in interorbital growth. The metopic suture which is open at birth fuses by one year of age. Growth at this suture increases the width of the interorbital region at an early age and permits growth of the cribriform plate of the ethmoid bone. The frontal-ethmoid suture fuses by two years of age. Growth of the internasal suture continues until adolescence when the perpendicular plate of the ethmoid eventually unites with it. Growth at the fronto-maxillary suture continues as long as the maxilla increases in size (Morin et al., 1963; Enlow, 1966; Enlow, 1982).

3. Appositional growth:

Appositional growth occurs concurrently with sutural growth and becomes more important after the sutures fuse. Enlow (1966), in a frontal cephalogram study, stated that the maxilla moves away from the cranium with bone growth in the maxillary-frontal suture. Periosteal bone deposition on the maxillary portion of the floor of the orbit functions to raise this area, thus adjusting the level of this area to the downward positioning of the maxilla. At the same time, bone deposition on the outward-sloping orbital floor serves to move the medial orbital wall in a distinctly lateral direction. In the opposite direction, resorption occurs in the zygomatic portion (lateral portion) of the orbital floor to produce a downward and lateral movement to keep it in line with the maxillary part of the orbit and results in enlargement of the orbital cavity. The medial part of the roof and the entire supraorbital rim are depository in nature . This regional remodeling pattern serves to lower the upper part of the orbit as an adjustment for new bone growth in a lateral direction. As a consequence of such relocation and remodeling adjustments, shape, alignment, and proportions are maintained.

4. Pneumatization:

Several air sinuses are located around the orbit. 1) The ethmoid air cells are the main structures affecting the interorbital dimension. At birth the ethmoid air cells occupy most of the lateral nasal wall. By age seven, the maxillary and ethmoid air cells each occupy half of the nasal wall. At ten years of age, the anterior and posterior ethmoid air cells develop toward the cribriform plate and encroach upon the frontal and sphenoid sinuses. Ossification of the ethmoid bone is not complete until seventeen years of age (Morin et al., 1963). 2) The frontal sinuses are not recognizable until age one. They expand superiolaterally to pass nasion and continue to expand into middle age. 3) The sphenoidal air sinuses in the posterior part of the interorbital region, continue to enlarge until three years of age. 4) The maxillary sinuses are small at birth but slow growth occurs until after adolescence.

5. Growth of the intraorbital structures:

Growth of the lacrimal glands and the extraocular muscles and the eyeball itself counteracts the above expanding forces. The eye increases three and one quarter times between birth and adulthood, with ninety percent of its growth occurring by seven years (Waitzman et al.,1992; Morin et al., 1963).

Morin et al (1963) concluded that interorbital width increase occurs as a combination of sutural growth, appositional growth as well as pneumatization of bones. The rapid phase of growth of the interorbital region persists until four years of age, one or two years after the closure of the fronto-ethmoid suture and actually before extensive pneumatization has taken place.

Overall harmonious intra and interorbital growth is a complex process and requires delicate compensatory adjustments among all the contributing structures. Any aberration in the process either pre or postnatally will cause orbital disproportion such as hypertelorism or hypotelorism. While there are several methods of defining orbital aberrations, there is no uniformly accepted approach to determine degree of involvement or amount of correction needed (Farkas, et al 1989). There are different methods to measure distance between the eyes : (1) those based on hard tissue boundaries of the bony orbits (Curranio and Silverman, 1960, Morin et al., 1963); (2) those based on soft tissue landmarks such as interpupillary distance and intercanthal distance (Farkas et al., 1992; Pryor, 1969); (3) either of the above adjusted for head size utilizing the ratio of intercanthal distance to head circumference (Costaras et al., 1982). Interorbital distance should be measured on the hard tissue or, less accurately, by measuring the distance between medial canthi. The interpupillary distance may not give a true indication of orbital hypertelorism because quite considerable exotropia is often present with ocular hypertelorism (Tessier 1972). Farkas et al. (1989) studied 63 Caucasian hypertelorism individuals to evaluate the relationship between surface intercanthal distance and skeletal orbital distance and suggested that surface measurements cannot replace skeletal measurement in planning for surgery. Rather, differences and relationships between soft-tissue and skeletal orbital measurements should be well understood to optimize surgical results.

The average interorbital distance between the right and left dacryon measurement on adult dried skulls was found to be 25 mm (Morin et al., 1963). Dacryon is the point where the frontal suture meets the nasal lacrimal suture. Whitnall, in 1932, recorded this distance as 21 mm, and the distance between the lacrimal points as 25.3 mm. The lacrimal point is at the junction of the upper border of the lacrimal bone and the posterior lacrimal crest. As described in Morin et al (1963), Hellman measured 78 Indian skulls in 1927 and found an overall average difference of 6.61 mm between infancy and senility. Ford, in 1958, examined 65 skulls of uncertain race and sex, and found an average size difference of 10 mm between birth and maturity. (Morin et al., 1963).

Determination of interorbital distance from standard postero-anterior cephalometric radiograph was introduced by Currarino and Silverman (1960). They measured medial orbital width using the point at the junction between each medial angular process of the frontal bone and the maxillary and lacrimal bone. P-A cephalograms have since been used by several authors for interorbital distance measurement (Athanasiou et al. 1992; Farkas et al., 1992; Costaras et al., 1982; Ishiguro, et al., 1976; Morin et al., 1963). Morin et al. (1963) in a mixed longitudinal study, found that overall growth in the interorbital region was 10 mm with 50 percent of interorbital growth occurring prior to three years of age. Costaras et al. (1982), also in a mixed longitudinal study using correction factor for P-A radiographic enlargement, found slow and steady increase in the interorbital region between 2 to 20 years of age. The average increase was 7 mm for both sexes. Growth in the females plateaued at approximately 14 years of age and at 16 for males. Athanasious et al. (1992) in a cross-sectional study of 588 children from 6 to 15 years of age, found that the interorbital distance increased by 4.5 mm.

More recently, CT scans were used to assess interorbital distance at several orbital levels. Waitzman et al (1992) in a cross sectional study of 542 normal subjects from 1 to 17 years of age, concluded that the overall size of the cranio-orbito-zygomatic skeleton reaches more than 85% of adult size by age 5 years. The medial interorbital distance changes little after birth, the lateral interorbital distance increases substantially in the first year of life and continues to grow throughout the growth period. However, no specific information about vertical height development was mentioned in any of these studies.

C. ORBITAL HYPERTELORISM AND THE RELATIONSHIP TO THE CRIBRIFORM PLATE

Orbital hypertelorism is a descriptive term indicating excessive distance between the orbits and hence the eyes. In 1924, Greig proposed the name hypertelorism for a deformity characterized by increased separation of the eyes (Costaras and Pruzansky, 1982). Tessier, in 1972, stated that hypertelorism is not an isolated finding, but part of malformations observed in several syndromes. Orbital hypertelorism appears secondary to many different malformations, the most frequent being facial clefts and those due to craniofacial dysostosis. At present, the term does not imply a single diagnostic entity but a finding in many clinical conditions caused by a number of factors (Costaras and Pruzansky, 1982).

The main anatomical characteristic of hypertelorism is a marked increase in width of the ethmoid sinuses (Converse et al., 1970). DeMyer et al. (1964) postulated a single mechanism that accounts for hypertelorism as part of a syndrome associated with median facial anomalies. He suggested that this factor was interference with the merging of structures along the median facial plane. The orbit is forced to remain at a fetal state because of the midline aberration associated with the facial clefts. However, since many of these syndromes differ in their pathogenecity, it may be assumed that orbital hypertelorism is produced by a variety of abnormal processes (Costaras and Pruzansky, 1982). In severe hypertelorism patients, the cribriform plate is often prolapsed. Tessier suggested the basis for the increased interorbital space was to be found in the cranial base, but did not explain the causative mechanism. Current interest in the surgical correction of orbital hypertelorism has been expanded to include spatial interrelationships with contiguous structures (Costaras and Pruzansky, 1982). Costaras and Pruzansky (1982) proposed several pathogenetic mechanisms for orbital hypertelorism:

1. Orbital hypertelorism may be caused by morphogenetic arrest such as facial cleft: such arrest would be manifested by failure of the orbits to move toward the medial due to some time-specific deficit in the process of differential growth (DeMyer et al., 1964). If this were the case, the initial interorbital distance would obviously be increased but there would be no reason to expect that future increase in interorbital distance would exceed the norm.
2. Orbital hypertelorism could be secondary to a primary midline lesion, such as a naso-encephalocele. The lesion would intervene in progressive medial approximation of the orbits during intrauterine development. If the midline lesion remained unchanged in size, the distance between the orbits would be expected to increase at a normal rate.
3. Orbital hypertelorism in premature craniosynostosis is caused by a different mechanism with an ongoing expansive process that separates the orbits during intrauterine development and continues through early postnatal growth. (Bertelsen, 1958; Tessier 1972; Tessier et al.,1973). It is a dynamic process, involving distortion of the cranial base secondary to craniosynostosis, that continues during early postnatal growth as part of accommodation to the growing brain within a selectively constricted neurocranium that expands and distorts at nonresistive points. This accommodation includes a downward deflection of the cribriform plate with expansion of the ethmoid air cells. When this is the case, the orbital hypertelorism would be expected to worsen during growth (Costaras and Pruzansky, 1982).

Median or paramedian facial clefts and orbital hypertelorism suggest a mechanism attributable to morphokinetic arrest. The increments for interorbital distance in craniofacial clefts should be similar or less than the norm (Costaras and Pruzansky, 1982).

Costaras et al. (1982), in a mixed longitudinal study of normal subjects, found that the level of the cribriform plate presented a progressively higher position relative to orbital height during growth but stabilized at about 14 years in the normal sample. In another study by Costaras and Pruzansky (1982) using the same method on 56 craniosynostosis and 31 facial cleft patients, it was confirmed that the facial cleft patients had similar increases in interorbital distance as the norms, while craniosynostosis patients showed greater increase. However, the cribriform plate level in both groups remained in a lower than normal position in relation to orbital height. In the present study, we utilize similar measurement in normal subjects to test for progressive change of the cribriform plate level in relation to orbital height during growth. It is expected that this information will be valuable in providing further diagnostic aid for cranial base and orbital aberrations.

D. OPTIMAL REFERENCE PLANE IN THE FRONTAL CEPHALOGRAM

Frontal cephalograms have become widely used for the study of transverse orbital dimensions and there has been general agreement to use crista galli as a midline reference. It is customary to divide the face by dropping a perpendicular from crista galli to a horizontal reference line. However, there has been no agreement concerning the horizontal reference plane for use in the P-A film. In searching the literature, very few studies have attempted to define the most reliable horizontal reference plane in the frontal film for accurate measurement of symmetry and spatial dimension.

Harvold (1954) found that the lateral limit of the zygomatic bone (fronto-zygomatic suture) is normally symmetric in relation to crista galli. Ishiguro et al. (1976) used the line connecting the medial point of the fronto-zygomatic suture as reference line for symmetry.

Ricketts used the line through the nasal septum or crista galli perpendicular to the line connecting the centers of the zygomatic arches to evaluate symmetry (Athanasiou, 1995). Svanholt and Solow (1977) used the perpendicular line through crista galli to the line connecting the intersection point of orbit and innominate points line. However, no empirical data have been presented to support the use of one reference plane above the others.

In the present study, we studied several reference lines and attempted to define the most stable horizontal reference line through time. With the advantage of the available maxillary implants in the longitudinal frontal films, the optimal reference line was defined as the one with which its perpendicular line through crista galli, oscillated the least relative to implant position.

III. SPECIFIC AIMS, HYPOTHESIS AND SIGNIFICANCE

This study is part of a general analysis of growth changes through time as seen on the longitudinal series of PA cephalograms of growing children with Björk-type implants gathered by Dr. Mathews in the Division of Orthodontics between 1967 and 1979. Information from these films have already been utilized in three dimensional studies of implant displacement through time (Korn and Baumrind, 1990) as well as for in progress studies of tooth eruption (Carlson et al., 1994) and bilateral symmetry (Frantz and Baumrind).

The primary focus of the current study is on growth changes in the region of the orbit. Data from the PA cephalograms will be analyzed with regard to three specific aims:

1. To obtain normative quantitative data on the central tendency and variability of orbital growth in the horizontal and vertical directions during growth.
2. To test the hypothesis of Pruzansky and coworkers that the level of the cribriform plate and the anterior cranial fossa migrate superiorly within the image of the orbit with growth .
3. To identify the optimal horizontal reference line of the film for use in interpreting PA cephalograms. The optimal line is defined as the line with respect to which the center of gravity of maxillary implants oscillates least through time.

This investigation makes use of the fact that the present data set is based on longitudinal records and takes particular advantage of the fact that maxillary implants are present in all cases in the sample.

It is believed that the findings will be useful for surgical teams in planning surgical intervention for patients with orbital disfiguration and thus to optimize the surgical outcome. Clinically, significant outcome would include:

1. The general growth pattern of the orbital cavity in transverse and vertical dimensions from 6 to 16 years.

2. Normative quantitative data on orbital cavity dimensions which will facilitate the treatment planning for major reconstructive procedures.
3. General normative relationship of the cranial base to the orbital cavity, providing baseline data on norms for use in further studies of pathogenetic condition.
4. The optimal reference plane in the frontal film which will facilitate further studies of asymmetries utilizing anterior-posterior cephalometric films.

IV. MATERIALS AND METHODS

A. SUBJECTS

The primary materials used in this study are cephalograms of 36 normal subjects taken at approximately annual intervals from age 6 years to 19 years. Subjects were recruited and records were collected by Dr. J. Rodney Mathews in the Section on Orthodontics, University of California School of Dentistry, during the years of 1967 to 1978 (Mathews and Ware, 1978). Under anesthesia, tantalum implants were placed bilaterally in the maxilla and unilaterally in the mandible of each child. A modified version of Björk's original pin setter was fabricated for placement of the tantalum pins that were 0.025 inch (0.64 mm) in diameter and approximately 1/16 inch (1.69 mm) long. All pins were driven to beneath the periosteum into the cortical bone (Mathews and Ware, 1978, Björk, 1968). Head films taken annually included P-A (frontal), norma lateralis (both in centric-relation and rest position), and 45-degree left and right oblique views (Mathews and Ware, 1978). In this study, P-A films of 20 cases with most timepoints available were used. Each case contained record at least 6 timepoints between 8 and 15 years (Table 1).

B. METHODS

1. IDENTIFICATION OF THE LANDMARKS

Trial experiments on two dry skulls were performed initially to identify and define landmarks to be used in this study. Lead pellets were fastened at specific landmarks and lateral and P-A cephalograms were taken. The P-A films were taken in three different head position for the purpose of identifying the influence of head rotation on the enlargement and localization of the landmarks. The three positions were: Frankfort horizontal (FH) plane parallel to horizon, upward rotation of 5 degrees and downward rotation of 5 degrees. After carefully identifying the relationship between the anatomic landmarks on the skull and the corresponding projections on the headfilms, a set of appropriate landmarks for the purpose of this study was identified. These landmarks are defined and shown in Table 2 and Figure 1.

Table 1. Distribution of cases and films.

Case No.		Sex	No. of TPs	Time points (TP) and nominal age (in years) at film date: 5.5	6.5	7.5	8.5	9.5	10.5	11.5	12.5	13.5	14.5	15.5	16.5	17.5	18.5
1		M	10		●	●	●	●	●	●	●	●	●		●		
2		M	11				●	●	●	●	●	●	●	●	●	●	●
3		M	10	●	●	●	●	●	●	●	●	●		●			
4		M	11		●	●	●	●	●	●	●	●		●	●	●	
5		F	9	●	●	●	●	●	●	●	●		●				
6	*	M	8				●	●	●	●	●	●	●	●			
7		F	8				●	●	●			●	●	●	●	●	
8		M	8				●	●		●	●			●	●	●	●
9		F	7			●	●		●		●	●	●	●			
10		F	9			●	●	●	●	●	●	●	●	●			
11	*	F	8		●	●	●	●	●	●	●		●				
12		F	9					●	●	●	●	●	●	●	●	●	
13		F	10			●	●	●	●	●	●		●	●	●	●	
14	*	F	9		●	●	●	●	●	●	●		●	●			
15	*	F	10			●	●	●	●	●	●	●	●	●	●		
16	*	F	11		●	●	●	●	●	●	●	●	●	●	●		
17	*	F	10			●	●	●	●	●	●	●	●	●	●		
18	*	M	10		●	●	●	●	●	●		●	●	●			●
19	*	M	10		●	●	●	●	●	●		●	●	●	●		
20	*	F	9		●	●	●	●	●	●		●	●	●			
Total				2	10	15	19	19	19	18	16	15	17	17	11	6	3
* total				0	6	8	9	9	9	9	6	7	9	8	4	0	0

* Subject used in reference line study.

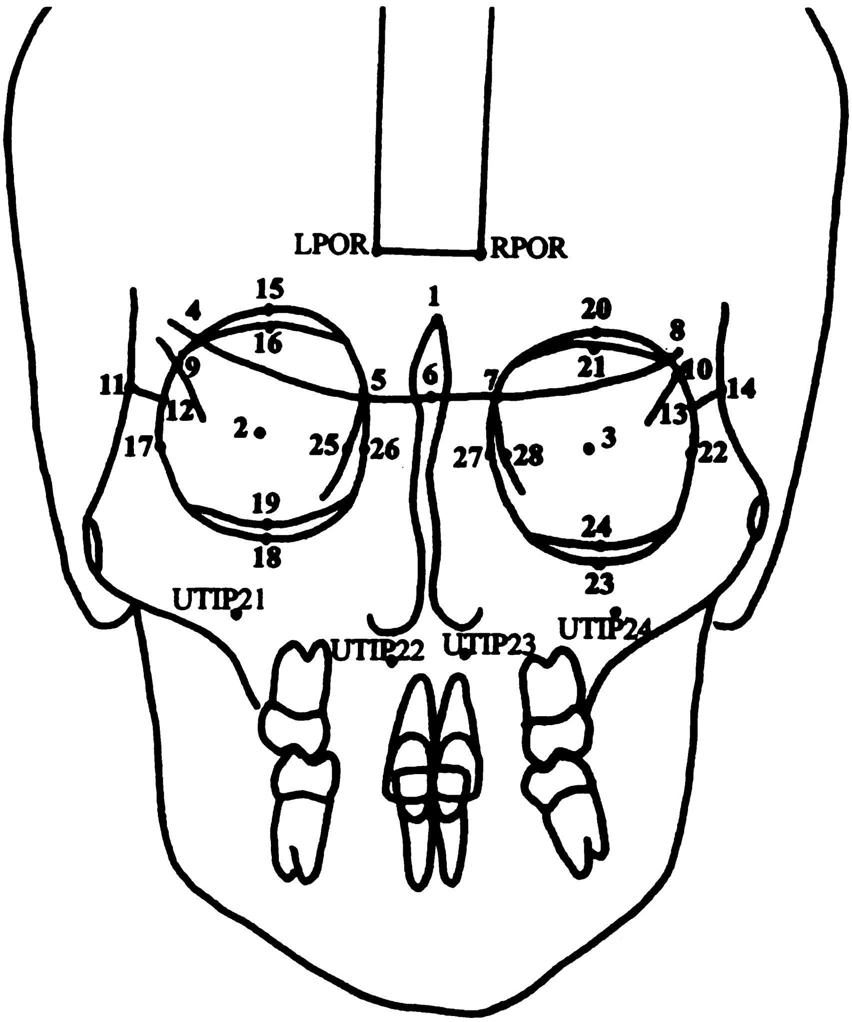

Figure 1. Cephalometric Landmarks

Table 2: Definition of Landmarks

1. CRISTAG (Crista Galli): The tip of crista galli
2. LOC (Left Orbitale Estimated Center): geometric center of outer contour of left orbit by visual inspection
3. ROC (Right Orbit Estimated Center): geometric center of outer contour of right orbit by visual inspection
4. LLFF (Left Lateral Fossa Floor): Intersection point of anterior cranial fossa @ left orbital lateral contour
5. LMFF (Left Medial Fossa floor): Intersection point of anterior cranial fossa @ left orbital medial contour
6. MIDFF (Middle Fossa Floor): Intersection point of anterior cranial fossa @ mid sagittal plane with crista galli
7. RMFF (right medial fossa floor): Intersection point of anterior cranial fossa @ right orbital medial contour
8. RLFF (Right Fossa Floor) : Intersection point of anterior cranial fossa @ right orbital lateral contour
9. LINOM (left innominate line): Intersection point of left innominate line, greater wing of the sphenoid bone, with left lateral orbital contour
10. RINOM (right innominate line): Intersection point of right innominate line, the greater wing of the sphenoid bone, with right lateral orbital contour
11. L_E_FZS (Left external Fronto-zygomatic Suture): lateral point on left fronto-zygomatic suture
12. L_I_FZS (Left internal Fronto-zygomatic zygo-frontal suture): medial point on left fronto-zygomatic suture
13. R_I_FZS (Right internal Fronto-zygomatic suture): medial point on right fronto-zygomatic suture
14. R_E_FZS (Right external Fronto-zygomatic suture): lateral point on right fronto-zygomatic suture

15. L_O_SUP1 (Left Superior Orbital Roof): Most superior point on roof of left orbital cavity
16. L_O_SUP2 (Left Superior Orbital Rim): most superior point on left orbital outer rim
17. LLR (Left Lateral Rim): most lateral point on left lateral orbital contour
18. L_O_INF1 (Left Inferior Orbital Floor): most inferior point on floor of left orbital cavity
19. L_O_INF2 (Left Inferior Orbital Rim): The most inferior point on the left inferior orbital rim
20. R_O_SUP1 (Right Superior Orbital Roof): Most superior point on right orbit roof
21. R_O_SUP2 (Right Superior Orbital Rim): most superior point on right superior orbital rim
22. RLR (Right Lateral Orbital Rim): most lateral point on right lateral orbital contour
23. R_O_INF1 (Right Inferior Orbital Floor): most inferior point on floor of right orbital cavity
24. R_O_INF2 (Right Inferior Orbital Rim): The most inferior point on right inferior orbital outer rim
25. LMO1 (Left Medial Orbital Point): the intersection of right and left lateral orbital line (17-22) @ left internal medial orbital rim
26. LMO2 (Left Medial Orbit Point): the intersection of the line connecting right and left lateral orbital points (17-22) @ medial orbital rim of left orbit
27. RMO2 (Right Medial Orbital Point): the intersection of the line connecting right and left lateral orbital points (17-22) @ medial orbital rim of right orbit
28. RMO1 (Right Medial Orbital Point):): the intersection of right and left lateral orbital line (17-22) @ right internal medial orbital rim

Table 2 (cont.):

Landmarks Added On Ten Films To Test The Optimal Reference Line

1. UTIP21: The geometric center of right upper maxillary implant.
2. UTIP22: The geometric center of right premaxilla implant
3. UTIP23: The geometric center of left premaxilla implant
4. UTIP24: The geometric center of left maxillary implant
5. LPOR: The left lower corner of the frontal head holder
6. RPOR: The right lower corner of the frontal head holder

2. TRACING AND DIGITIZING OF LANDMARKS

i). Digitizing of orbital landmarks

The tracing and digitizing were performed with the computer-aided head film analysis system at UCSF (Baumrind and Miller, 1980). All the films have four fiducials, A, B, C and D on the four corners, prepared with the same template. The fiducials are used for within-film superimposition. The landmarks traced are demonstrated in figure 1 and defined in table 2. The four corner fiducial points were included in the beginning of the tracing point list. Each film was traced twice by the investigator, with all cases traced once, and then followed by the second tracing. The two tracings of each film were then digitized utilizing the UCSF computer-aided system. By anatomic coordinate-loading software, the two tracings of each film were superimposed automatically using the corner fiducials. Thus the mean of every landmark of the two tracings was computed. If any landmark identification from the two tracings on each film fell beyond the 95% confidence level envelope (Baumrind and Frantz, 1971a), a third tracing and digitizing of the specific landmark and the four corner fiducials were repeated. By superimposing on the corner fiducials again, the computer would automatically choose the two closest among the three measurements of the specific landmark which fell inside the 95% confidence envelope and average the data. If three tracings of the same landmark in the same film were separated beyond the envelope, that landmark was considered ambiguous enough to be discarded and the data were not included in the analysis.

ii). Input of the maxillary implant landmarks

After digitizing films of 20 cases with all the orbital landmarks, it was decided to add the maxillary implant landmarks and the landmarks of the corners of the cephalometric forehead holder in ten of the cases (table 1, figure 1 and table 2). The purpose of this addition was to identify the most stable reference frame for evaluating changes through time. These procedures were conducted entirely on a computer operation using digital images of the headfilms which had been scanned with Agfa Arcus #II digital scanner (Agfa division, Bayer Co. Wilmington) at a spatial resolution of 300 dpi and gray scale resolution of 8 bit. For the purpose of landmark identification on the screen, a specialized software based on NIH image 1.45 was utilized. It was specified by Dr. Baumrind and developed by Mr. Frederic Ti, MSEE, as courtesy to CRIL. After digitizing, the information of the maxillary implants was merged with previously acquired information as described in section A by superimposing all data on the common corner fiducials in the analogue mode described above.

3. ERRORS OF METHOD

Errors of measurement are usually of two types - systematic error and random error. Systematic errors involve the error of x-ray machine set up, error of radiographic technique, different head posture between different films and the enlargement factor in the headfilms. The second is the error of identification, which involves tracing error, digitizing error and machine error in point location (Baumrind et al., 1983a; Houston, 1983).

Frontal films have errors of projection which are also encountered with lateral projection. Both head positions share problem of projection displacement (enlargement), but the problems of rotation of the head around the ear rod axis are more severe in frontal films. Rotation around ear rod axis in lateral films affects all points in the skull equally. For this reason, lateral films differing in rotation are geometrically similar and can be superimposed accurately simply by rotation of the films. With frontal headfilms, on the other hand, downward rotation of the anterior part of the face is coupled with upward rotation of the posterior part. For this reason, frontal films generated at different degree of cranial rotation are not geometrically similar and are not likely superimposable. Added to this problem, there is another problem of change of enlargement factor by growth. Because of the increasing skull dimensions in a growing individual, the orbital plane gets closer to the film, and consequently the enlargement of orbital structures gets smaller. This problem also exists in lateral cephalograms, but to a much smaller degree.

Because of these differential enlargement factors in different planes in the frontal film, the measurements have inherent inaccuracies. The original plan for this study was to construct a three-dimensional geometric map correcting for errors in the transverse dimension of frontal films through use of information from the lateral films taken at the same visit. Performing this task with this sample would have been somewhat facilitated by the presence of metallic implants, but the complicated task could not be accomplished with the available time and resources.

Various methods have been used in the past to analyze x-ray images of the craniofacial region. Broadbent first developed a biplanar method for three-dimensional x-ray stereometry. The method involved one frontal and one lateral head film taken nearly simultaneously from a pair of x-ray tubes so oriented that: (1)the angle of intersection between their central rays was 90 degrees. (2) the subject to be examined was placed at the point of intersection (3) two film cassettes were used, each oriented perpendicular to the other and to the central ray of the emitter (Broadbent, 1931; Brodie, 1949; Baumrind et al, 1983a). The Broadbent method provided a perfect idea but several technical difficulties have prevented its practicality for clinical use (Baumrind et al., 1983a,b):

1. The problem of landmark identification is consequential. To obtain accurate three-dimensional information, it is essential to identify the same landmark unambiguously on both frontal and lateral images. However, it is actually very challenging to identify the same point on both lateral and frontal headfilms with acceptable degree of confidence (Baumrind et al., 1983a). This task is remarkably difficult in this study since the images of most of the anatomic structures in the orbital area in which we are interested differ markedly in shape and discernibility between the two projections. This was verified by the lateral and frontal images of the dry skulls with lead pellets in the trial experiment. For example, the Orbitale we determined on the lateral film was not the same point we would identify as Orbitale on the frontal film and it also differs from skull to skull.
2. It is difficult to compensate for the difference in enlargement of structures which lie at different distances from the frontal and lateral film surfaces. If the skull is placed in planes parallel to the film plane, the enlargement factor for distances measured between points in any given plane will be the same, while the enlargement factor in the other

planes will be different. If the subject's head has been rotated 90 degrees between the films, the line segment lying in the three planes in each figure is differentially enlarged. Thus, the enlargement factor for any given anatomic landmark will differ from the lateral projection to the frontal projection unless by coincidence the structure happens to be the same distance from both the lateral and the frontal film surfaces.

3. In the materials used in this study, the frontal and lateral films were obtained sequentially and not simultaneously. Therefore, potentially different head rotation would further complicate the problem of differential enlargement.

From these points of view, the reconstruction of " Three-dimensional" information involves technical difficulties which are beyond our current capabilities. Putting the information of frontal and lateral films together is a real problem in this biplanar system and has not been resolved yet. The solution might be possible using the coplanar method of Baumrind (Baumrind et al, 1983a,b), or through the use of 3D scans such as CT or MRI. However, these methods have their own problems of precision, irradiation and high cost.

With respect to errors of identification, the difficulty in identifying the landmarks actually varies from point to point (Baumrind and Frantz, 1971a). An important factor responsible for this is the sharpness of the viewed edge, that is the degree to which the edge contrasts with the surrounding area. Those points which lie within the confines of the skull have a greater likelihood of being confounded by "noise" from adjacent or superimposed structures. This accounts for the difficulty in accurately locating the points in the orbital area in the frontal film which overlap with other levels of craniofacial structures. However, identification of points such as the center of the orbit turned out to be readily and accurately accomplished. This was done by visual estimation (Baumrind and Frantz, 1971a). The human performance in identifying the center of a structure by visual estimation is usually quite good since it involves mental averaging of multiple points.

Our strategies for minimizing these identification errors included: (1) Before landmark identification was determined, we took trial frontal films on two dry skulls with lead pellets on the landmarks around the orbital cavity and examined carefully the correspondence of the pellet images on the frontal films and the skulls. (2) Double determinations of all landmarks were made and averages used to decrease the measurement error. (Baumrind and Frantz, 1971a). (3) Sampling of multiple cases was done at multiple timepoints.

4. MEASUREMENT

Aim 1. Changes in interorbital distances and in height and width

Seven measurements were used to evaluate the height and width of the right and left orbit separately and the horizontal distance between the right and left orbits. Detailed definitions of the points used and dimensions measured are shown in Figure 2, 3, 4 and Table 3.

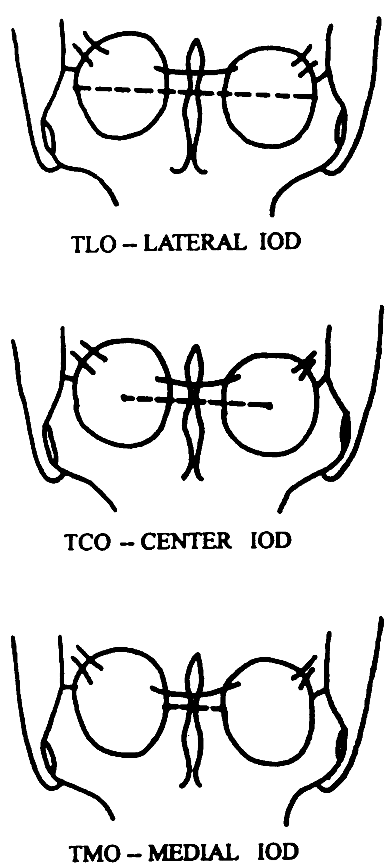

Figure 2. Interorbital Distance Measurement

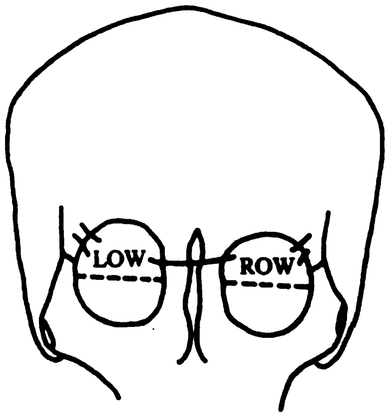

Fig 3. Orbital Width Measurement

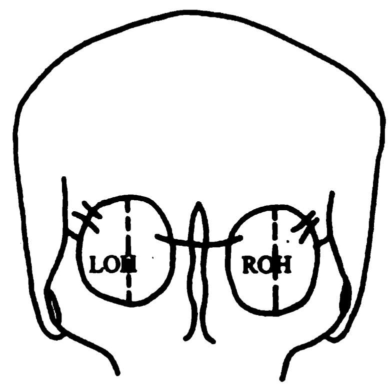
Fig 4. Orbital Height Measurement

Table 3: Interorbital Distance, Orbital width and Height Measurement

Interorbital Distances

1. TMO: (LMO2-RMO2), The distance between the most medial points of orbital cavities
2. TLO: (LLR-RLR), The distance between the most lateral points of orbital cavities
3. TCO: (LOC-ROC), The distance between the centers of orbital cavities

Orbital Widths

4. LOW: Left orbital width (LLR-LMO2), The distance between the most lateral and medial points of left orbit
5. ROW: Right orbital width (RLR-RMO2), The distance between the most lateral and medial points of left orbit

Orbital Heights

6. LOH: Left orbital height (LOSUP1-LOINF1), The distance between the most superior and inferior points of left orbit
7. ROH: Right orbital height (ROSUP1-ROINF1), The distance between the most superior and inferior points of right orbit

Aim 2. The level of the cribriform plate relative to orbital height

The method used to measure the vertical position of the cribriform plate relative to orbital height was that of Costaras and Pruzansky (1982). The distance between the most superior point (LOSUP1) and inferior point (LOINF1) of the left orbit connotated left orbital height. The same procedure was used for the right side. A line parallel to the line between the two orbital centers was drawn through MIDFF (representative of level of cribriform plate, Figure 5). This line divided the orbital height into upper and lower portion and the ratio between the upper portion and total orbital height was calculated. The right and left ratios and the averages were analyzed.

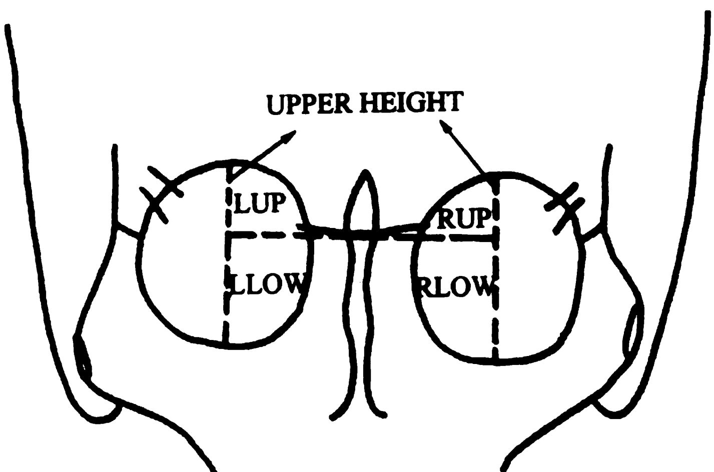

$$\text{LOCP} = \frac{\text{UPPER HEIGHT}}{\text{TOTAL HEIGHT}}$$

Figure 5. Level of Cribriform Plate Relative to Orbital Height

Aim 3. The optimal horizontal reference line in the frontal film

The most optimal reference line in the frontal film is defined as the line with which its perpendicular line through crista galli, oscillates the least relative to the maxillary implants. The tested line was designated as the x axis, while the crista galli perpendicular represented the y axis. The intersection point of the crista galli perpendicular to the tested line was used as the origin. The implant reference was defined as the center of gravity of the four maxillary implants, which was calculated by averaging the x and y values of the implants (Figure 6). The distance of the implant center was measured in x and y values relative to the reference line and the reference perpendicular line for every timepoint. The data and graphs are reported as the difference of the x value of the reference film to every time point from age 7 to 15. The same principle was applied to the y value. Six reference lines were tested by this method (Figure 7 and Table 4).

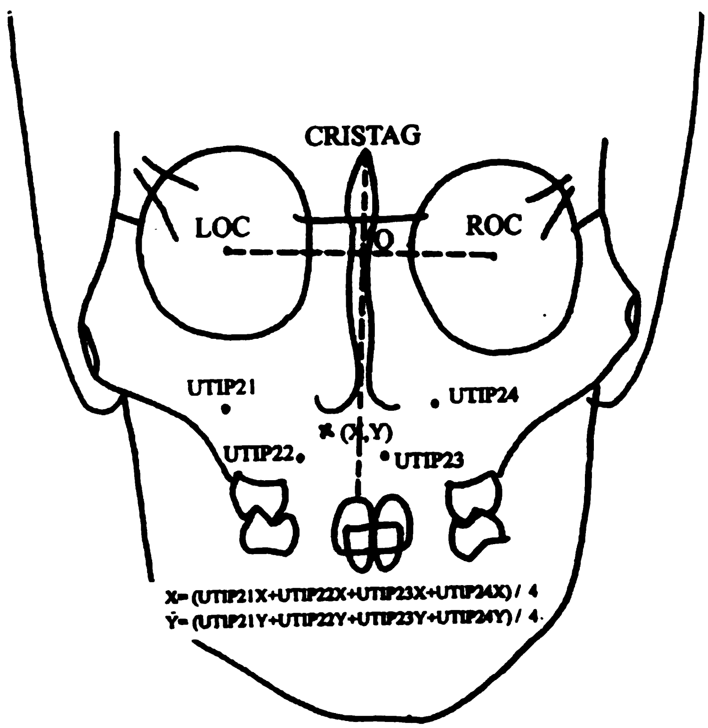

Figure 6. Implant Displacement Relative to Reference Line

Table 4: The Six Tested Reference Lines

1. **LPOR - RPOR: Horizontal line of frontal head holder (as representing of machine horizontal line)**
2. **LLFF - RLFF: The line connecting the intersection points of anterior fossa floor with orbital lateral contour**
3. **LINOM - RINOM: The line connecting the innominate points - the intersection points of greater wing of sphenoid with orbital lateral contour**
4. **LEFZS - REFZS: The line connecting the lateral points of fronto-zygomatic suture**
5. **Line connect LIFZS and RIFZS: The line connecting the medial points of fronto-zygomatic suture**
6. **LOC - ROC: The line connecting the center points of the orbits**

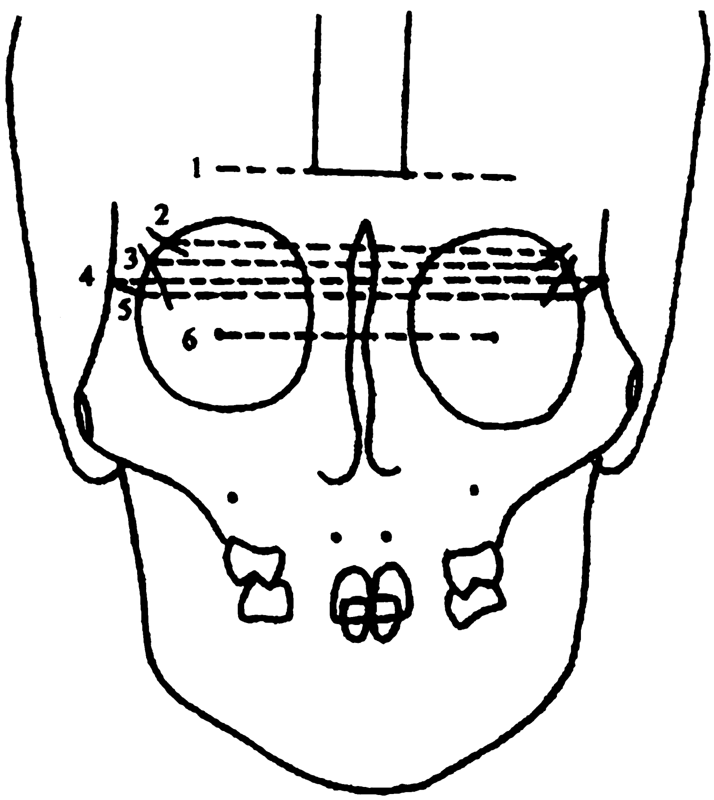

Figure 7. Six Tested Reference Lines

V. RESULTS

A. GROWTH OF THE BONY ORBIT

Data were obtained to describe growth change of the bony orbit in transverse and vertical dimensions from age 5 to 18 years. The sample size, mean and standard deviations of the six measurements at each time point are presented in table 5. Data from 6 to 16 are graphically displayed in figure 8, 9 and 10. Data before age 6 and after 16 are not included due to small sample size. The three figures present increases in interorbital distances and right and left orbital cavity width and height.

All measurements show small but steady increases with age and no obvious growth spurt. As seen in Table 5 and Figure 8, the distance between the landmarks on the lateral orbital rim (TLO) increased more than the distance between the medial points (TMO) or the center points (TOC).

Figure 9 shows that the increase in right and left orbital width was gradual and leveled off after 14 years of age. The right orbital width appeared slightly bigger than the left side, however, there was no significant difference between the two sides.

In Figure 10, it is seen that orbital height also increased by small increment , about the same amount as orbital width, from 6 to 16 years. It should be noted that the standard deviations tend to be larger for the height than for the width measurement.

AGE	N	TMO		TCO		TLO		LOW		ROW		LOH		ROH	
		MEAN	STD	MEAN	STD	MEAN	STD	MEAN	STD	MEAN	STD	MEAN	STD	MEAN	STD
5	2	21.1	3.2	58.2	1.0	87.8	/	33.6	2.0	34.0	/	39.9	3.2	41.3	1.4
6	7	21.8	2.3	57.5	2.0	88.7	2.5	33.1	1.7	33.8	1.8	39.7	1.9	40.1	1.5
7	14	21.8	1.9	57.3	2.2	88.9	3.5	33.2	1.3	34.0	1.8	40.4	1.8	39.4	3.2
8	17	21.4	1.8	57.7	2.1	89.2	2.8	33.7	1.3	34.1	1.6	40.0	1.8	40.0	1.8
9	18	22.5	2.2	59.1	2.2	91.0	2.6	34.2	1.2	34.3	1.4	39.9	2.3	40.3	1.9
10	20	22.4	2.1	59.1	2.7	91.5	3.9	34.3	1.5	34.8	2.0	40.5	2.4	40.4	2.3
11	17	23.7	2.1	60.5	2.8	93.4	4.1	34.7	1.5	34.9	1.8	40.5	2.2	40.4	2.2
12	16	23.6	2.7	60.8	3.3	93.5	4.4	34.7	2.1	35.2	1.8	40.5	2.9	40.6	2.7
13	17	24.1	2.3	61.3	3.2	94.4	4.1	34.9	1.5	35.3	1.8	41.2	3.0	41.0	3.2
14	18	24.3	2.3	62.1	2.8	96.3	4.0	35.8	1.5	36.1	2.1	41.3	2.7	40.2	2.3
15	18	24.3	2.5	62.3	3.1	96.5	3.9	36.0	1.3	36.2	1.2	42.2	2.8	41.4	2.4
16	8	25.6	3.1	63.6	4.1	97.5	5.7	35.7	1.6	36.1	2.1	42.4	2.6	42.1	3.7
17	4	24.9	2.4	62.1	2.6	97.9	6.4	36.7	3.4	36.3	3.1	41.1	1.4	40.8	1.5
18	1	24.4	/	59.5	/	91.6	/	33.5	/	33.8	/	37.4	/	37.2	/
19	1	28.6	/	66.1	/	/	/	36.3	/	/	/	40.6	/	40.9	/

Table 5. Measurements of Interorbital Distances, Orbital Widths and Heights

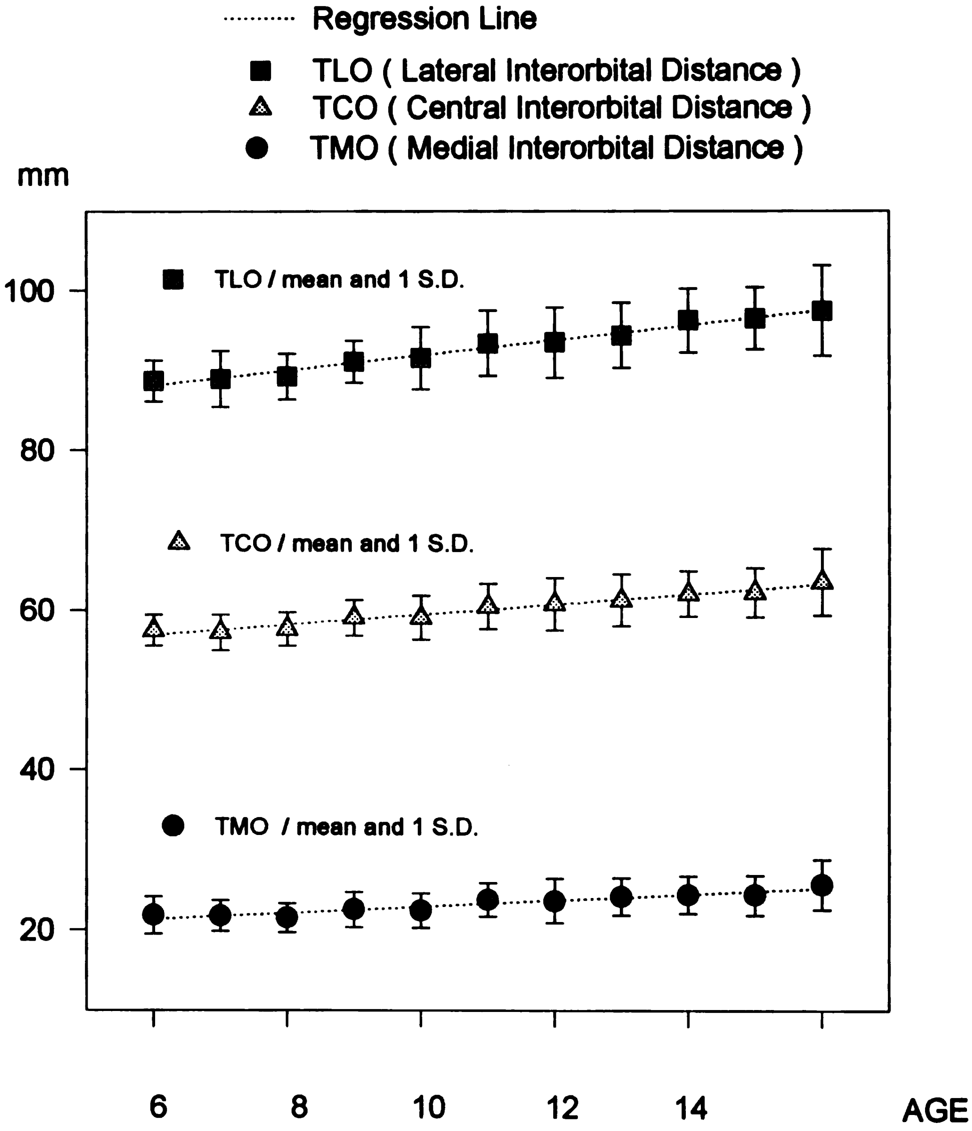

Figure 8. Interorbital Distance / Regression Lines

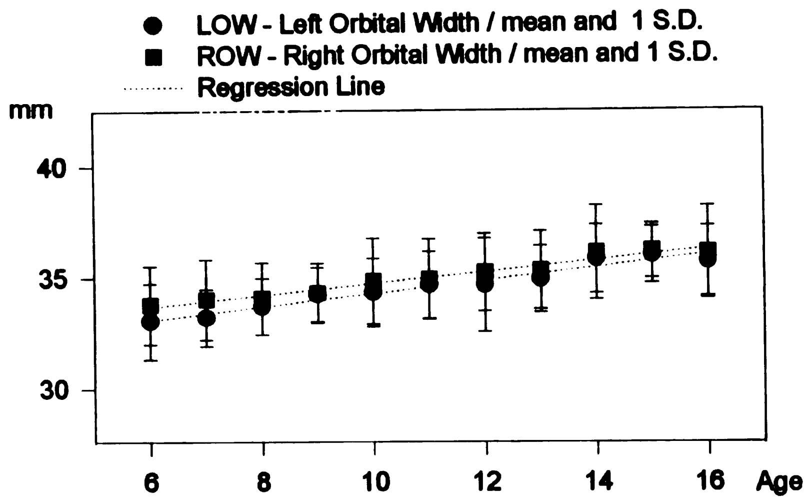

Figure 9. Orbital Width / Regression Lines

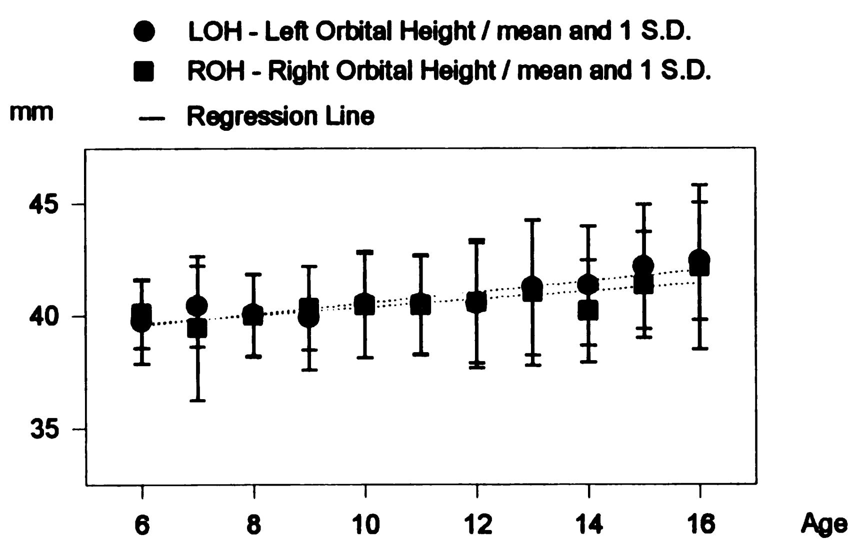

Figure 10. Orbital Height / Regression Lines

B. LEVEL OF CRIBRIFORM PLATE RELATIVE TO THE ORBITAL HEIGHT

Data were analyzed to show possible change of the level of the cribriform plate relative to total orbital height during growth. Table 6 shows the means and standard deviations of the upper and lower height of the right and left orbit, as well as the ratio of upper orbital height to total orbital height. It was found that the upper orbital height stayed constant in size on both sides. On the other hand, the lower orbital height increased slowly from 6 to 16 years.

The cribriform plate was projected in the upper third of the orbit on both sides throughout the growth period studied. The percentage of upper orbital height relative to overall height showed a slight tendency to decrease with age as seen in Figure 11.

This indicated that the level of the cribriform plate relative to the overall orbital height rises slightly with age. However, the large variation and large standard deviations must be noted.

AGE	N	Left Upper		Left Lower		Right Upper		Right Lower		Left Upper Orbital Height Ratio		Right Upper Orbital Height Ratio		Mean of Upper Orbital Ratio	
		Mean	Std dev	Mean	Std Dev	Mean	Std Dev	Mean	Std Dev	Mean	Std Dev	Mean	Std Dev	Meam	Std Dev
5	2	15.1	0.9	24.8	4.1	16.1	1.7	24.9	2.9	38.1	5.4	39.4	5.3	38.7	5.3
6	7	15.5	2.1	24.1	2.8	15.0	1.5	24.9	2.1	39.2	5.7	37.7	3.9	38.5	4.8
7	14	15.0	1.9	25.4	3.1	13.6	4.2	25.6	2.6	37.2	5.5	34.1	10.3	35.7	7.4
8	18	15.1	2.2	24.9	2.5	14.8	2.4	25.1	2.2	37.7	5.3	37.1	5.6	37.4	5.4
9	18	15.0	1.7	24.9	2.4	14.3	2.3	25.8	2.2	37.7	4.2	35.7	5.3	36.7	4.7
10	20	15.1	2.0	25.3	2.8	14.2	2.1	26.1	2.7	37.4	4.8	35.4	5.1	36.4	4.9
11	17	15.0	2.1	25.5	2.5	14.4	2.1	25.9	2.4	37.0	4.9	35.7	4.8	36.3	4.8
12	16	14.1	1.8	26.4	3.2	13.5	1.8	26.9	3.1	35.0	4.6	33.5	4.6	34.2	4.6
13	17	14.1	2.2	27.0	3.4	13.4	2.5	27.5	3.6	34.4	5.6	32.8	6.0	33.6	5.7
14	18	14.9	2.1	26.3	2.8	14.2	2.1	25.9	2.8	36.2	4.8	35.4	5.2	35.8	5.0
15	18	15.5	2.0	26.7	2.4	14.6	2.4	26.7	2.4	36.7	4.1	35.3	5.3	36.0	4.5
16	8	15.2	1.2	27.2	2.5	14.5	1.6	27.5	3.4	35.9	2.8	34.6	3.9	35.3	3.3
17	4	15.5	1.1	25.5	0.4	15.1	0.9	25.5	1.3	37.8	1.3	37.1	2.0	37.4	1.1
18	1	11.6	/	25.8	/	10.5	/	26.6	/	31.1	/	28.2	/	29.7	/
19	1	14.5	/	25.8	/	14.8	/	26.0	/	36.5	/	36.2	/	36.4	/

Table 6. Measurements of Upper, Lower Orbital Heights and Upper Orbital Height Ratio

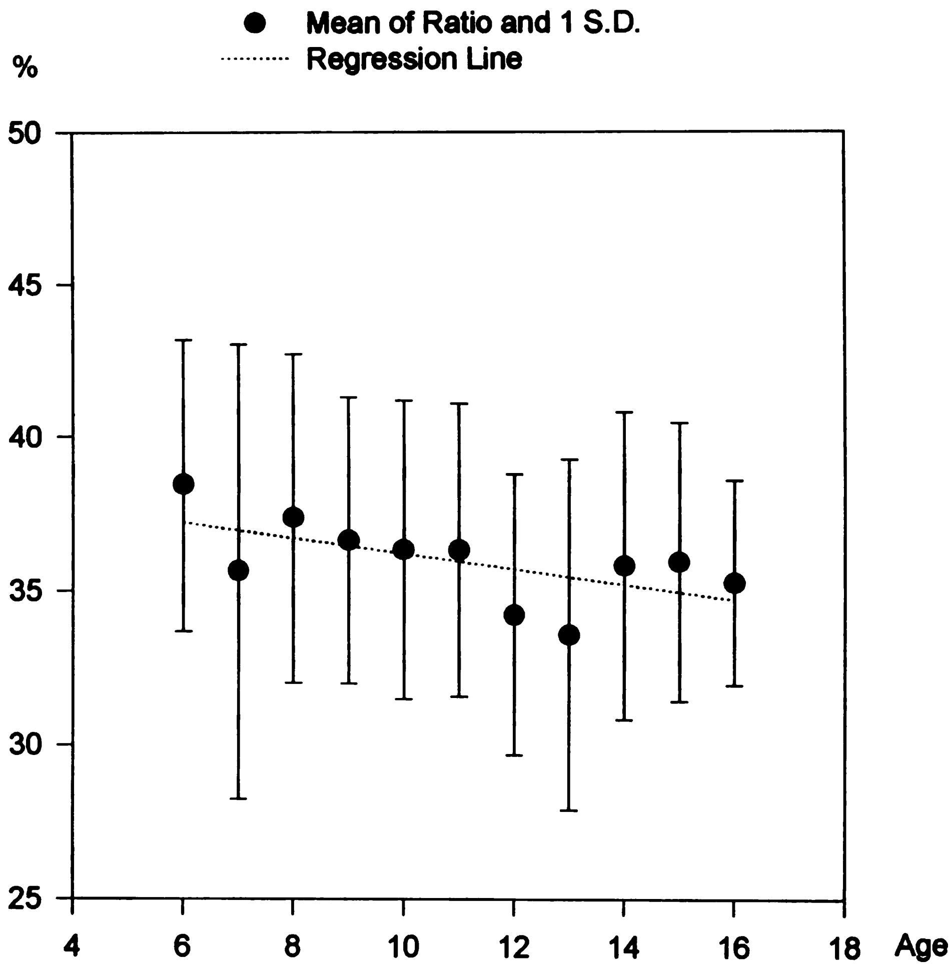

Figure 11. Level of Cribriform Plate Relative to Orbital Height / Regression Line

C. THE OPTIMAL REFERENCE LINE ON THE FRONTAL FILM

Data on displacement of the center of gravity of the four maxillary implants in the horizontal plane as x values and in the vertical plane as y values are presented in Table 7 and 8 respectively. Sample size at each time point is presented in the first column. The x and y mean values in each column are presented as the difference from the value of the reference age (age 12) and the value of each time point (from age 5 to age 19). Figure 12 presents graphically the displacement of the implant center in the horizontal direction (x axis) relative to the crista galli perpendicular line of each tested reference line from age 7 to age 15. Data before age 7 and after age 15 are excluded in the figures due to small sample size. The means and standard deviations were plotted separately to offer clearer view of the degree of the implant gravity center at the different ages relative to the reference line. The line which has the least zigzag pattern and least variability (smallest standard deviations) represents the most stable reference line.

The data given in Table 7 and the graphs presented in Figure 12 show that most of the reference lines were quite stable relative to the maxillary implants. The horizontal line of the head holder (# 1) showed the greatest variation. The line connecting the center of the orbit (# 6) also demonstrated some wobbling, indication variation relative to the stable implant markers. The straightest line with the smallest standard deviations and consequently the most stable reference line, was the line connecting the two innominate points (# 3). The line connecting the external points (# 4) and the line connecting the internal points (# 5) of the fronto-zygomatic sutures demonstrated very similar standard deviations and were both relatively stable during growth.

AGE	LPOR-RPOR			LLFF-RLFF			LINOM-RINOM			LEFZS-REFZS			LIFZS-RIFZS			LOC-ROC		
	Frame of reference #1			Frame of reference #2			Frame of reference #3			Frame of reference #4			Frame of reference #5			Frame of reference #6		
	N	Mean	Std Dev	N	Mean	Std Dev	N	Mean	Std Dev	N	Mean	Std Dev	N	Mean	Std Dev	N	Mean	Std Dev
T12-T6	3	-2.3	0.3	3	0.3	0.4	3	-0.2	0.6	3	0.7	0.8	3	0.8	0.2	3	0.2	0.1
T12-T7	3	0.4	3.9	4	0.4	0.6	4	0.0	0.7	4	0.1	1.1	4	0.7	0.7	4	0.4	1.4
T12-T8	6	-0.7	2.7	7	-0.1	0.5	7	-0.1	0.4	7	0.2	0.7	7	0.6	0.9	7	0.1	0.9
T12-T9	6	-1.1	0.7	7	0.2	0.5	7	-0.1	0.7	7	0.1	0.5	7	0.4	0.6	7	0.2	1.2
T12-T10	8	-1.0	2.4	8	0.5	1.0	8	0.2	0.7	8	0.4	0.7	8	0.7	0.8	8	0.0	1.4
T12-T11	8	-0.5	2.0	8	0.2	0.6	8	-0.1	0.6	8	0.3	0.6	8	0.3	0.7	8	0.4	0.8
T12-T12	6	0.0	0.1	6	0.0	0.1	6	-0.1	0.1	6	0.2	0.4	6	0.2	0.4	6	0.0	0.1
T12-T13	6	0.6	0.8	6	0.1	0.7	6	0.1	0.4	6	0.0	0.5	6	0.4	0.6	6	-0.3	0.7
T12-T14	6	0.4	1.7	6	-0.5	0.9	6	-0.4	0.5	6	0.5	1.0	6	0.5	1.0	6	0.3	0.7
T12-T15	5	0.4	0.8	5	0.2	0.4	5	0.0	0.5	5	0.3	0.8	5	0.7	0.9	5	0.1	0.6
T12-T16	2	3.0	5.2	2	4.1	6.4	2	3.8	6.2	2	4.3	4.9	2	4.5	4.8	2	3.6	5.8
T12-T17	0	/	/	0	/	/	0	/	/	0	/	/	0	/	/	0	/	/
T12-T18	1	9.6	/	1	7.7	/	1	8.3	/	1	7.7	/	1	7.2	/	1	6.5	/

Table 7. Horizontal Displacement of Gravity Center of Maxillary Implants Relative to Reference Lines.

AGE	LPOR-RPOR			LLFF-RLFF			LINOM-RINOM			LEFZS-REFZS			LIFZS-RIFZS			LOC-ROC		
	Frame of reference #1			Frame of reference #2			Frame of reference #3			Frame of reference #4			Frame of reference #5			Frame of reference #6		
	N	Mean	Std Dev	N	Mean	Std Dev	N	Mean	Std Dev	N	Mean	Std Dev	N	Mean	Std Dev	N	Mean	Std Dev
T12-T6	3	8.5	2.6	3	3.7	1.1	3	4.4	1.3	3	3.7	2.6	3	3.6	2.6	3	2.4	0.9
T12-T7	3	5.9	1.8	4	4.5	1.2	4	5.2	1.6	4	4.8	2.3	4	3.8	2.0	4	4.1	1.6
T12-T8	6	6.0	1.3	7	3.0	0.9	7	3.7	1.3	7	3.3	1.8	7	2.8	1.6	7	2.2	1.6
T12-T9	6	4.1	1.6	7	2.1	1.2	7	2.6	1.2	7	3.0	1.1	7	2.6	1.1	7	1.5	1.2
T12-T10	8	3.5	4.0	8	1.2	0.8	8	1.6	1.0	8	1.5	1.7	8	0.8	1.6	8	0.8	0.9
T12-T11	8	1.8	2.4	8	0.4	0.7	8	0.5	1.0	8	0.5	1.1	8	0.2	1.0	8	0.3	0.6
T12-T12	6	0.1	0.3	6	-0.2	0.4	6	-0.1	0.2	6	-0.8	2.1	6	-0.8	2.0	6	-0.2	0.4
T12-T13	6	-0.6	2.6	6	-0.7	1.0	6	-0.9	1.0	6	-0.7	1.8	6	-1.2	1.8	6	-0.7	0.9
T12-T14	6	-1.6	1.9	6	-1.1	1.3	6	-1.1	1.1	6	-1.8	3.5	6	-1.5	2.9	6	-1.0	1.3
T12-T15	5	-0.3	3.1	5	-1.7	1.4	5	-1.9	1.3	5	-2.1	2.0	5	-1.7	1.9	5	-1.7	1.7
T12-T16	2	1.8	2.3	2	-4.3	1.7	2	-4.8	1.3	2	-5.5	2.5	2	-4.4	2.2	2	-3.9	0.9
T12-T17	0	/	/	0	/	/	0	/	/	0	/	/	0	/	/	0	/	/
T12-T18	1	5.6	/	1	-6.2	/	1	-7.2	/	1	-6.2	/	1	-5.8	/	1	-5.8	/

Table 8. Vertical Displacement of Gravity Center of Maxillary Implants Relative to Reference Lines.

Figure 12. **Variability of Implant Displacement as a Function of Alternative Frames of Reference**

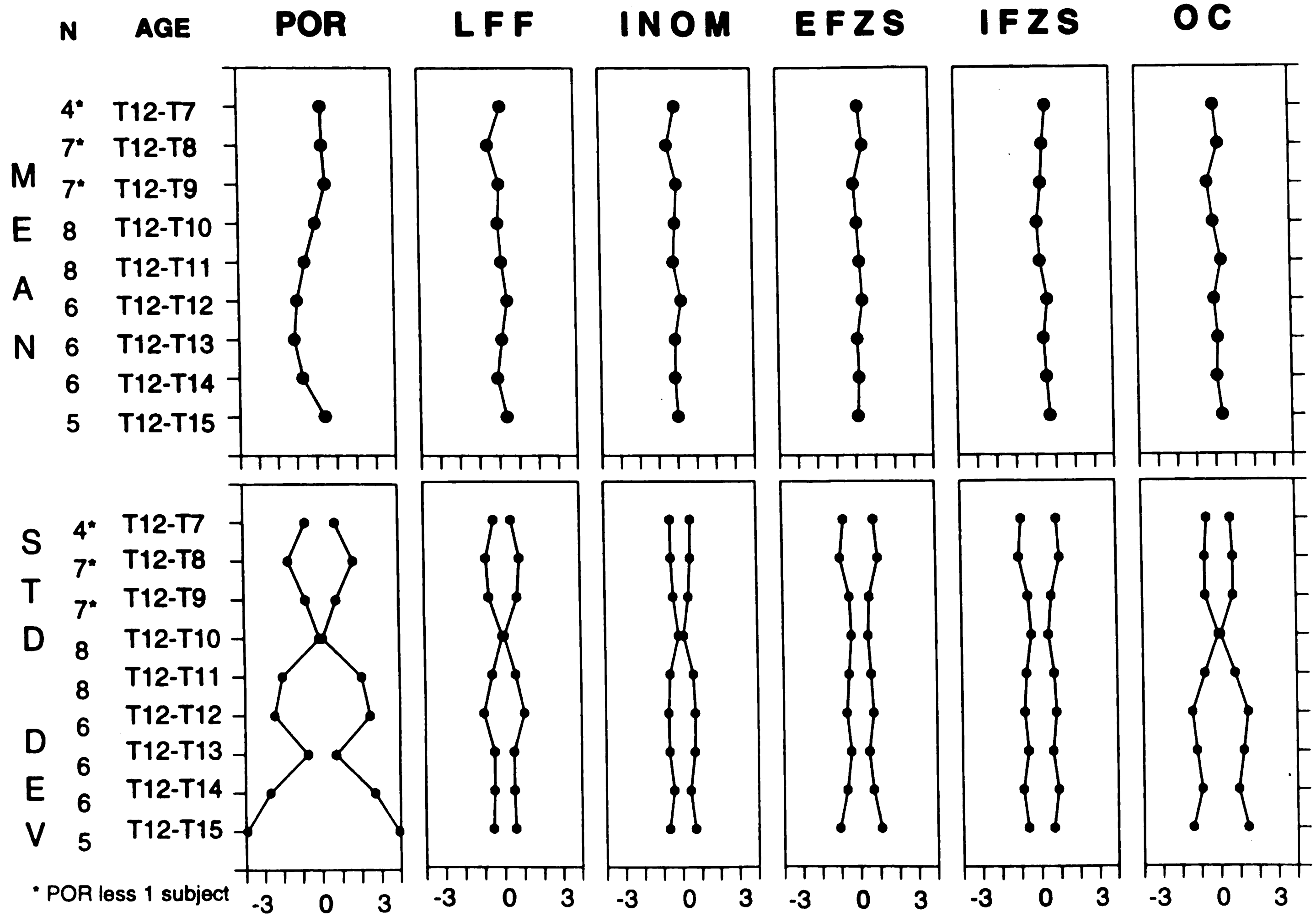

* POR less 1 subject

VI. DISCUSSION

A. ENLARGEMENT FACTORS, HEAD POSITION

In recent years there has been a growing demand for extensive roentgenographic control material as a result of refinement in syndrome identification and the desire to improve treatment of craniofacial anomalies. One of the areas where information is scant is the orbital region. Although radiographs have been used to assess interorbital distance, accurate measurements of the orbital region on frontal cephalograms is difficult due to the inherent geometric magnification, distortions and variations in head position, leading to difficulties in superimposition on anatomical structures (Baumrind and Frantz, 1971; Athanasiou, 1995, Karskov et al., 1997). Munro and Das (1979) have criticized the use of frontal headfilms for assessing hypertelorism. Their criticism was based on the argument that a two-dimensional approach was being utilized to assess a three-dimensional problem. With respect to the enlargement distortion, Farkas et al. (1989) suggested using an 8% enlargement factor for all frontal films. Besides the enlargement factor inherent from the geometry, height measurements are affected by up-and-down rotation of the head while horizontal measurements are influenced by right and left head rotation. It is difficult to obtain consecutive cephalograms in a standardized manner with the same head position, especially vertically (Athanasiou et al., 1992). However, Ishiguro et al.(1976) studied geometric change on the P-A headfilms in various head position, and found that a change within 10 degrees of up-down or right-left rotation resulted in a difference less than the method error and was a negligible factor in width measurement. Costaras et al. (1982) found lateral rotation up to 20 degrees and vertical rotation up to 10 degrees did not change the measurement significantly. In our trial experiments, a small and a large skull with lead beads on the landmarks were used to test variation in measurement due to positioning. Frontal films of each skull were taken in three different vertical angulation: horizontal plane parallel to the floor, upward turn of 5 degrees and downward turn of 5 degrees. It was found that the orbital height measurements were minimally affected by this variation in vertical head position.

The effect of the differential enlargement factor becomes reduced with growth as the orbital plane gets closer to the film cassette. Due to the fact that calculating the enlargement factors of structures at different levels relative to the film plane would be exceedingly complicated, no attempt was made to correct for this in this study. As the differential enlargements decrease with age, any detected measurement difference between time points would indicate real change.

Computed tomography does not have the problem of anatomic superimposition and differential enlargements (Kargskov et al., 1997; Waitzman et al., 1992). However, cost factors preclude the use of computerized tomography for the assessment of interorbital distance in large samples. Kargskov et al. (1997) compared the reliability of anatomic points recorded from conventional cephalometry and 3-D CT using nine human skulls. They found no evidence that the 3-D CT is more reliable than the conventional cephalometric methods in normal skull. They suggest that 3-D CT would be valuable in assessing severe asymmetries.

B. GROWTH OF THE BONY ORBIT

1. CHANGES IN INTERORBITAL DISTANCES

Growth assessment by means of PA cephalograms is complicated by lack of well-defined stable structures for superimposition of subsequent cephalogram tracings (Athanasiou, 1995). Despite inherent difficulties in obtaining accurate measurement from frontal films, our data are similar to those obtained by others where corresponding parameters were assessed.

The medial interorbital distance increased from 21.8 mm (SD=2.3 mm) to 25.6 mm (SD=3.1 mm) from 6 to 16 years. These findings correspond to most of the published norms on interorbital distances. Although various different medial landmarks have been used in other studies, the results are very similar (Currarino and Silverman, 1960; Morin et al., 1963; Athanasiou et al., 1992). Similar results are also reported in Costaras et al. (1982) cephalometric study using enlargement correction factor and Waitzman et al. (1992) study using cross-sectional CT scans.

No obvious growth spurt or plateau was noted in the growth curve of interorbital distance in this age group. Morin et al. (1963) in a mixed longitudinal study, including younger age groups starting from newborn, concluded that there was about 10 mm overall growth in medial interorbital distance with 50% of the growth occurring prior to three years. After three, the rate of growth decreased but continued in a slow steady fashion. Waitzman et al. (1992) in a cross-sectional study of CT scans found that the cranial vault grows rapidly in the first year of life but growth levels off early. The upper midface grows at a slower rate in infancy, but continues to grow later in childhood and early adolescence. They concluded that the cranio-orbital-zygomatic skeleton reaches more than 85% of its eventual adult size by age 5 years. From those findings, it would be reasonable to expect a much steeper growth curve before 6 years of age, the age group not included in this study.

Increase in interorbital distance after age 16 is expected to be very small. The mean interorbtial distance at age 16 in the present study is very close to the value of an adult control group in Morin et al. study (1963), and also to the value of a group of 20 years old in Costaras et al. study (1982). Unlike long bones and the mandible, significant growth in the upper craniofacial skeleton in late adolescence, after age 16 is expected to be minimal (Waitzman et al., 1992).

2. CHANGES IN ORBITAL WIDTH AND HEIGHT

The most superior point of the orbital outline in the frontal film does not represent the orbital rim, but rather the orbital roof, as identified by the lead beads in our trial experiments on skulls. The same applies to the inferior point of the orbit. Therefore, the measurements of orbital height represent measurements of the bony orbit. The data showed that increase in width and height are small, gradual and proportional from age 6 to 16. However, the standard deviations are higher for the height measurement than for the width measurement. This can at least in part be explained by variation in vertical head position. Krogman (1979) found that growth in the width of the jaws tends to be complete before the adolescent growth spurt and is affected minimally, if at all, by adolescent growth changes. Furthermore, he stated that growth in width is completed first, then growth in length, and finally growth in height. This is different from the parallel growth pattern of height and width of the bony orbit. The orbital cavity grows to accommodate the growth of the globe which has insignificant change of size and shape after early in life. The globe, as part of the neurocranium, increases three and one quarter times between birth and adulthood, with ninety percent of its growth occurring before seven years of age (Morin et al., 1963).

Taking this information together, it appears that the orbit serves as a bridge between the neurocranium and the viscerocranium with its growth following closer to that of the neurocranium than of the lower face. Most of its growth is completed early in life before age six, and only small increments of growth continues until at least late adolescence, maintaining harmonious relationships between the neurocranium and the viscerocranium.

C. LEVEL OF THE CRIBRIFORM PLATE RELATIVE TO ORBITAL HEIGHT

Costaras and Pruzansky (1982) studied normal subjects from age 2 to 20 years and proposed that the level of the cribriform plate relative to orbital height (represented by the ratio of upper to total orbital height) decreases with age indicating superior migration of the level of cribriform plate relative to orbital height as measured on frontal films. They found negligible increase with age in the part of the orbit above the cribriform plate level. The decreasing upper orbital height ratio relative to the total orbital height was interpreted as a consequence of downward and forward displacement of the inferior orbital margin. This follows the growth of the maxilla into adolescence, while the cribriform plate remains relatively fixed as part of the neurocranium where growth stabilizes at a much earlier age in keeping with the neural growth curve (Costaras et al., 1982). Similar results are found in the present study with minimal growth in both right and left upper orbital height above the cribriform plate level. The small increases of right and left lower orbital height were responsible for the overall increase in height. This supports the view of the orbit providing an adjustment zone between the neurocranium and the midface.

Although the mean ratio of upper orbital height to overall orbital height demonstrated a slight tendency to decrease with age as seen in Figure 11, it is not significant and the standard deviations are large. Thus, a superior migration of the cribriform plate level during this growing period was not confirmed. Due to small overall increases in orbital height from 6 to 16 years of age, the level of the cribriform plate would not be expected to change significantly. In the Pruzansky study, the obvious "rise" of cribriform level relative to orbital height occurred in an age group younger than ours although their data did show that the level continued to rise slowly during later growth as well.

Due to the fact that these measurements involve constructed points relating two different spatial levels of structures: orbital and anterior cranial base, they are very sensitive to changes in up-down head rotation. This may be the main reason for the large standard deviations seen. Although superior migration of the cribriform plate level during this growing period could not be confirmed in this study, there still may be value in using these parameters to study differences of the upper orbital height ratio between norms and individuals with craniosynostosis syndromes.

D. THE MOST OPTIMAL HORIZONTAL REFERENCE LINE

Frontal film have been primarily used to study transverse dimension and symmetrical pattern. Different reference lines have been used in different studies as mentioned above (Ricketts et al., 1972; Svanholt and Solow, 1977; Harvold, 1954; Ishiguro et al., 1976). However, no rigorous study on stability or reliability of reference frame has been reported.

With the advantage of maxillary implants in the longitudinal frontal film used in this study, the most reliable reference line is defined as the line which with respect to the perpendicular through crista galli varies the least relative to the center of gravity of the implant markers from one time period to the next. Slight asymmetric growth of maxilla is expected in a normal population. This would be expected as a horizontal displacement (x value) of the maxillary implant gravity center relative to the reference perpendicular line and the line would progressively deviate from the perpendicular line. However, as long the mean horizontal displacement of the implant center relative to the reference line stays constantly linear without wiggling in its path, it is considered to be a reasonably stable reference line through time.

Seen from the results, there is a similar pattern of the means and standard deviations of horizontal displacement of the implant gravity center between the line connecting the intersection point of the orbital cavity and the anterior cranial fossa, and the line connecting the intersection point of the orbital cavity and the innominate line- the greater wing of the sphenoid bone intersection with the lateral orbital contour. This is a reasonable finding as these two lines are very close in location and both represent intersection points with the cranial base. Judging the overall pattern by visual inspection of the graph, it is seen that the line connecting the innominate points, due to its stability and least variability relative to maxillary implants, is the most preferable line as reference frame in the frontal film. However, this line actually involves a virtual point constructed by intersection of two different spatial planes, which can be seen only in the frontal film but which does not exist as a real anatomic structure. As a consequence, the identification of this point will be influenced by up-down head rotations. Hence, although this line is recommended for reference frame for horizontal measurements, its reliability as reference frame to study vertical measurement needs further investigation. To further accurately define the most reliable reference line, larger sample size and a statistical test of variability would be needed.

The reference lines connecting the external points and internal points of the fronto-zygomatic suture also present very similar patterns both in the means and standard deviations in horizontal displacement of implant gravity center. This is reasonable since this is a pair, of inner and outer side, of the same anatomic structure. This pair of points demonstrates reasonable reliability as demonstrated by the minimal oscillation and reasonable distribution of variation. However, these two points are not easy to identify in some frontal film with compromised quality, and this might account for the wider variation compared to the line connecting the innominate points.

The line of the forehead holder had the poorest quality as reference line as it demonstrated an obviously wobbled curve and wide variation relative to the implant markers. This indicates that one cannot expect the ear rod holder to align the head in a constant position at intervals during growth. The line connecting the geometric center of the orbit is also not recommended as a reliable reference line due to its zigzag pattern relative to the implant markers through time and the relatively wide variation. Since this line is constructed by visual inspection, larger variation than a clear anatomic point is expected.

VII. CONCLUSIONS

Growth changes of the orbital cavity in 20 normal children with maxillary implants were studied from age 6 to 16 years. The findings include :

1. All measurements of interorbital distances demonstrated slow but steady increases. There were also small but symmetrical increases in height and width of both right and left orbit.
2. On average, there was no increase in upper orbital height above the cribriform plate level, but a small increase in lower orbital height. The level of the cribriform plate lies on average in the upper third of the orbital image, but the variation was large. There was no obvious tendency of superior migration of the cribriform plate level relative to the orbital image on frontal film from 6 to 16 years of age. Thus Pruzansky's hypothesis was not confirmed in this sample of normal subjects.
3. The line connecting the intersection point of the orbital cavity and the innominate point was found to be the most reliable horizontal reference line on the frontal film since it demonstrated the most stability and least variability relative to the maxillary implants through time. In contrast, the horizontal line of the head holder was the least reliable reference line. The conclusions relative to the reliability of the reference lines are tentative because of small sample size. Further investigation using a larger sample should be undertaken.

VIII. REFERENCES

Apt, L. and S. Isenberg (1973). Changes in orbital dimensions following enucleation. Arch Ophthalmol **90**(5): 393-5.

Athanasiou, A. E. (1995). Orthodontic cephalometry. London, Mosby-Wolfe., pp:140-162, 181-202.

Athanasiou, A. E., H Droschl and C. Bosch (1992). Data and patterns of transverse dentofacial structure of 6- to 15-year-old children: a posteroanterior cephalometric study. AM J Orthod **101**(5): 466-471.

Baumrind, S. and R. C. Frantz (1971). The reliability of head film measurements. 1. Landmark identification. Am J Orthod **60**(2): 111-27.

Baumrind, S. and R. C. Frantz (1971a). The reliability of head film measurements. 2. Conventional angular and linear measures. Am J Orthod **60**(5): 505-17.

Baumrind, S. and F. Moffitt (1972b). Mapping the skull in 3-d. J Calif Dent Assoc **48**(2): 22-31.

Baumrind, S. and D. M. Miller (1980). Computer-aided head film analysis: the University of California San Francisco method. Am J Orthod **78**(1): 41-65.

Baumrind, S., F. H. Moffitt, and Curry S. (1983a). Three-dimensional x-ray stereometry from paired coplanar images: a progress report. Am J Orthod **84**(4): 292-312.

Baumrind, S., F. H. Moffitt, and Curry S. (1983b). The geometry of three-dimensional measurement from paired coplanar x-ray images. Am J Orthod **84**(4): 313-22.

Baumrind, S., E. L. Korn, and Y. Ben-Bassat (1987a). Quantitation of maxillary remodeling. 2. Masking of remodeling effects when an anatomical method of superimposition is used in the absence of metallic implants. Am J Orthod Dentofacial Orthop **91**(6): 463-74.

Baumrind, S., E. L. Korn, Y. Ben-Bassat, and E. E. West (1987b). Quantitation of maxillary remodeling. 1. A description of osseous changes relative to superimposition on metallic implants. Am J Orthod Dentofacial Orthop **91**(1): 29-41.

Bertelsen, T. (1958). The premature synostosis of the cranial sutures. Acta Ophtal **Suppl 51**:1-175.

Björk, A. (1968). The use of metallic implants in the study of facial growth in children: method and application. Am J Phys Anthropol **29**(2): 243-54.

Broadbent B. H. (1931). A new x-ray technique and its application to orthodontia. Angle Orthod **1**(2): 45-66.

Brodie, A. G. (1949). Cephalometric roentgenology: history, technics and used. J Oral Maxillofac Surg 7(3): 185198.

Bu, B., L. B. Kaban, and K. Vargervik (1989). Effect of Le Fort III osteotomy on mandibular growth in patients with Crouzon and Apert syndromes. J Oral Maxollofac Surg **47**: 666-671.

Carlson, S, CF.A. Moorrees, and S. Baumrind (1994). Eruption patterns in the human mandible studied with Björk implants. Harvold Scholl of Dentistry, Senior thesis. Counway Medical Library, Harvard University.

Coccaro, P. J., J. G. McCarthy, F. J. Epstein, D. Wood-Smith, and J. M. Converse (1980). Early and late surgery in craniofacial dysostosis: a longitudinal cephalometric study. Am J Orthod 77(4): 421-36.

Converse, J. M., J. Ransohoff, E. S. Mathews, B. Smith, and A. Molenaar (1970). Ocular hypertelorism and pseudohypertelorism: advances in surgical treatment. Plast Reconstr Surg **45**:1-13.

Costaras, M. and S. Pruzansky (1982). Bony interorbital distance (BIOD), head size, and level of the cribriform plate relative to orbital height: II. Possible pathogenesis of orbital hypertelorism. J Craniofac Genet Dev Biol **2**(1): 19-34.

Costaras, M., S. Pruzansky, and B. H. Broadbent Jr. (1982). Bony interorbital distance (BIOD), head size, and level of the cribriform plate relative to orbital height: I. Normal standards for age and sex. J Craniofac Genet Dev Biol **2**(1): 5-18.

Currarino, G., F. Silverman (1960). Orbital hypertelorism, arrhinencephaly and trigononcephaly. Radiology **74:** 206-217.

DeMyer, W., W. Zeman, and C. G. Palmer (1964). The face predicts the brain: diagnosis significance of median facial anomalies for holoprosencephaly (arhinencephaly). Pediatrics **34**: 226-263.

Enlow, D. H. (1966). Morphogenetic analysis of facial growth. Am J Orthod **52**(4): 283-99.

Enlow, H. D. (1982). Handbook of facial growth. 2nd ed. Philadelphia: WB Sanders.

Farkas, L. G., R. B. Ross, J. C. Posnick, and G.D. Indech (1989). Orbital measurements in 63 hypertelorism patients. Differences between the anthropometric and cephalometric findings. J Craniomaxillofac Surg **17**(6): 249-54.

Farkas, L. G., K. J. C. Posnick, T. M. Hreczko, and G. E. Pron (1992). Growth patterns in the orbital region: a morphometric study. Cleft Palate Craniofac J **29**(4): 315-318.

Frantz, R. C., and S. Baumrind. Bilateral facial asymmetry studied longitudinally on posteroanterior cephalograms. In preparation for submission to the Angle Ortnod.

Hansman, C. F. (1966). Growth of interorbital distance and skull thickness as observed in roentgenographic measurements. Radiology **86**(1): 87-96.

Harvold, E. (1954). A roentgen study of the postnatal morphogenesis of the facial skeleton in cleft palate. Oslo. Anatomical institute, University of Oslo. pp:11-18, 82-83.

Hogeman, K. E. and K. Willmar (1974). The Le Fort III osteotomy for Crouzon's disease in children. Report of a four-year follow-up in one patient. Scand J Plast Reconstr Surg **8**(1-2): 169-72.

Houston, W. J. B. (1983). The analysis of errors in orthodontic measurements. Am J Orthod **83**(5): 382-390.

Iseri, H. and B. Solow (1990). Growth displacement of the maxilla in girls studied by the implant method. Eur J Orthod **12**(4): 389-98.

Iseri, H. and B. Solow (1996). Continued eruption of maxillary incisors and first molars in girls from 9 to 25 years, studied by the implant method. Eur J Orthod **18**(3): 245-56.

Ishiguro, K., W. M. Krogman, M. Mazaheri, and R. L. Hardin (1976). Longitudinal study of morphological craniofacial patterns via P-A x-ray headfilms in cleft patients from birth to six years of age. Cleft Palate J **13**: 104-26.

Kargskov, J., C. Bosch, C. Gyldensted, and S. Sindet-Pedersen (1997). Comparison of the reliability of craniofacial anatomicc landmarks based on cephalometric radiographs and three-dimensional CT scans. Cleft Palate J **34**(2): 111-116.

Korn, E. L. and S. Baumrind (1990). Transverse development of the human jaws between the ages of 8.5 and 15.5 years, studied longitudinally with use of implants. J Dent Res **69**(6): 1298-306.

Kreiborg, S. (1981). Craniofacial growth in plagiocephaly and Crouzon syndrome. Scand J Plast Reconstr Surg **15**(3): 187-97.

Kriens, O. (1974). Maxillary osteotomy in early childhood. A preliminary report. J Maxillofac Surg **2**(2-3): 150-2.

Krogman, W.M. (1979) Craniofacial growth, prenatal and post natal. In: Cooper HK ed. Cleft palate and cleft lip: a team approach to clinical management and rehabilitation. Philadelphia: WB Saunders Co., pp:22-107.

Lee, Y., K. Vargervik and S. Baumrind. Orbital growth in juveniles. In preparation

Lejoyeux, E., J. F. Tulasne, and P. L. Tessier (1986). Maxillary growth following total septal resection in correction of orbital hypertelorism. Cleft Palate J **23 Suppl 1**: 27-39.

Limborgh, J. and I. Tonneyck-Muller (1976). Experimental studies on the relationships between eye growth and skull growth. Ophthalmologica **173**(3-4): 317-25.

Mathews, J. R. and W. H. Ware (1978). Longitudinal mandibular growth in children with tantalum implants. Am J Orthod **74**(6): 633-55.

McCarthy, J. G., P. J. Coccaro, F. Epstein, and J. M. Converse (1978). Early skeletal release in the infant with craniofacial dysostosis: the role of the sphenozygomatic suture. Plast Reconstr Surg **62**(3): 335-46.

Morin, J. D., J. C. Hill, J. E. Anderson, and R. M. Grainger (1963). A study of growth in the interorbital region. Am J Ophthal **56**: 895-901.

Moore, L. K. P., T.V.N. (1993). The developing human, Clinically orientated embryology. Philadelphia, W. B. Saunders Co.

Munro, I. R. (1978). The effect of total maxillary advancement on facial growth. Plast Reconstr Surg **62**(5): 751-62.

Munro, L. R., and S. K. Das (1979). Improving results in orbital hypertelorism correction. Ann Plast Surg **2**: 499-507.

Pryor, H. B. (1969). Objective measurement of interpupillary distance. Pediat **44**: 973-977

Ricketts R. M., R. W. Bench, J. J. Hilgers, and R. Schulhof (1972). An overview of computerized cephalometrics. Am J Orthod **61**: 1-28.

Sarnat, B. G. and P. D. Shanedling (1972). Orbital growth after evisceration or enucleation without and with implants. Acta Anat (Basel) **82**(4): 497-511.

Sarnat, B. G. (1978). Differential craniofacial skeletal changes after postnatal experimental surgery in young and adult animals. Ann Plast Surg **1**(2): 131-45.

Spolyar, J. L., W. Vasileff, and R. B. Machintosh (1993). Image corrected cephalometric analysis (ICCA): design and evaluation. Cleft Palate Craniofac J **30**(6): 528-39.

Svanholt, P., and B. Solow (1977). Assessment of midline discrepancies on the posteroanterior cephalometric radiograph. Trans Eur Orthod Soc **25**: 261-8.

Tessier, P. (1972). Orbital hypertelorism. I. Successive surgical attempts. Material and methods. Causes and mechanisms. Scand J Plast Reconstr Surg **6**(2): 135-55.

Tessier, P., G. Guiot and P. Derome (1973). Orbital hypertelorism. II. Definite treatment of orbital hypertelorism (OR.H.) by craniofacial or by extracranial osteotomies. Scand J Plast Reconstr Surg **7**(1): 39-58.

Waitzman, A. A., J. C. Posnick, D. C. Armstrong, and G. Pron (1992). Craniofacial skeletal measurement based on computed tomography: part II. Normal values and growth trends. Cleft Palate J **29**(2): 118-128.

Wei, S. H. (1970). Craniofacial width dimensions. Angle Orthod **40**(2): 141-7.

Whitnall, S. E. (1932). Anatomy of the Human Orbit. London, Oxford, 1932, ed. 2.

Zide, M. B. J. W. G. (1985). Surgical Anatomy of the Orbit, Raven Press.

IX. APPENDIX

Table 9. Measurements of Interorbital distances, orbital widths and heights

N Obs	Variable	N	Minimum	Maximum	Mean	Std Dev
20	STUDY_01	20	9505.00	9505.00	9505.00	0.00
	CASE_01	20	1.00	33.00	15.55	10.48
	TP_01	20	23.00	28.00	25.95	1.57
	SEX_01	20	1.00	2.00	1.50	0.51
	AGE_01	20	11.13	13.07	12.41	0.46
	TMO_01	20	19.24	29.55	23.83	2.59
	TLR_01	20	83.37	99.50	93.72	4.02
	TOC_01	20	53.25	66.52	60.95	2.89
	LOW_01	20	30.28	39.59	34.66	1.93
	ROW_01	20	31.76	38.70	35.24	1.62
	LOH_01	20	36.23	45.37	40.73	2.62
	ROH_01	20	36.72	45.92	40.52	2.49
	CASE_02	20	1.00	33.00	15.55	10.48
	TP_02	2	21.00	21.00	21.00	0.00
	SEX_02	2	1.00	2.00	1.50	0.71
	AGE_02	2	5.13	5.94	5.54	0.57
	TMO_02	2	18.82	23.36	21.09	3.21
	TLR_02	1	87.84	87.84	87.84	.
	TOC_02	2	57.54	58.90	58.22	0.96
	LOW_02	2	32.21	35.04	33.63	2.00
	ROW_02	1	33.98	33.98	33.98	.
	LOH_02	2	37.64	42.21	39.92	3.23
	ROH_02	2	40.27	42.30	41.28	1.44
	CASE_12	20	0.00	0.00	0.00	0.00
	TP_12	2	-7.00	-7.00	-7.00	0.00
	SEX_12	2	0.00	0.00	0.00	0.00
	AGE_12	2	-7.39	-6.90	-7.14	0.35
	TMO_12	2	-7.04	-6.19	-6.62	0.60
	TLR_12	1	-9.52	-9.52	-9.52	.
	TOC_12	2	-7.62	-5.92	-6.77	1.20
	LOW_12	2	-2.09	0.00	-1.04	1.48
	ROW_12	1	-2.47	-2.47	-2.47	.
	LOH_12	2	-3.37	-3.16	-3.27	0.15
	ROH_12	2	-3.62	-0.27	-1.94	2.37
	CASE_03	20	1.00	33.00	15.55	10.48
	TP_03	7	21.00	22.00	21.29	0.49
	SEX_03	7	1.00	2.00	1.43	0.53
	AGE_03	7	6.38	7.07	6.78	0.23
	TMO_03	7	18.36	25.26	21.83	2.31
	TLR_03	7	84.13	90.65	88.65	2.53
	TOC_03	7	53.90	59.73	57.49	1.95
	LOW_03	7	31.64	35.88	33.05	1.71
	ROW_03	7	30.79	35.49	33.78	1.76
	LOH_03	7	37.95	43.24	39.72	1.85
	ROH_03	7	37.67	41.72	40.09	1.54
	CASE_13	20	0.00	0.00	0.00	0.00
	TP_13	7	-7.00	-5.00	-6.00	0.58
	SEX_13	7	0.00	0.00	0.00	0.00
	AGE_13	7	-6.31	-4.93	-5.85	0.44
	TMO_13	7	-7.51	-0.36	-3.59	2.22
	TLR_13	7	-9.36	-4.13	-7.10	2.06
	TOC_13	7	-7.71	-4.12	-5.33	1.21
	LOW_13	7	-5.80	0.83	-1.71	2.24
	ROW_13	7	-3.21	-1.04	-1.79	0.72
	LOH_13	7	-5.61	2.58	-2.02	2.61

TP 01: Refernce age 12.   TP 02-09: Age 5-12

N Obs	Variable	N	Minimum	Maximum	Mean	Std Dev
20	ROH_13	7	-4.39	0.94	-2.16	1.86
	CASE_04	20	1.00	33.00	15.55	10.48
	TP_04	14	21.00	23.00	21.71	0.73
	SEX_04	14	1.00	2.00	1.57	0.51
	AGE_04	14	7.03	7.97	7.61	0.25
	TMO_04	14	18.38	25.24	21.75	1.89
	TLR_04	14	84.00	94.21	88.90	3.47
	TOC_04	14	54.59	61.17	57.26	2.22
	LOW_04	14	31.70	35.88	33.20	1.28
	ROW_04	14	30.95	37.05	34.01	1.81
	LOH_04	14	37.53	43.98	40.41	1.81
	ROH_04	14	30.48	43.98	39.44	3.20
	CASE_14	20	0.00	0.00	0.00	0.00
	TP_14	14	-6.00	-3.00	-4.86	0.95
	SEX_14	14	0.00	0.00	0.00	0.00
	AGE_14	14	-5.66	-3.59	-4.87	0.58
	TMO_14	14	-4.84	2.12	-2.47	1.95
	TLR_14	14	-8.74	2.15	-5.50	2.78
	TOC_14	14	-6.36	-2.37	-4.43	1.30
	LOW_14	14	-5.24	0.84	-1.60	1.62
	ROW_14	14	-3.89	1.31	-1.37	1.24
	LOH_14	14	-4.55	3.25	-0.97	2.00
	ROH_14	14	-10.10	2.09	-1.60	2.95
	CASE_05	20	1.00	33.00	15.55	10.48
	TP_05	18	21.00	24.00	22.50	0.99
	SEX_05	18	1.00	2.00	1.44	0.51
	AGE_05	18	8.04	8.99	8.52	0.25
	TMO_05	17	18.87	25.48	21.44	1.77
	TLR_05	17	83.63	93.59	89.20	2.83
	TOC_05	18	54.84	62.00	57.68	2.11
	LOW_05	17	31.69	35.81	33.70	1.28
	ROW_05	17	30.77	37.21	34.06	1.62
	LOH_05	18	35.99	44.25	40.02	1.81
	ROH_05	18	37.36	44.28	39.98	1.83
	CASE_15	20	0.00	0.00	0.00	0.00
	TP_15	18	-5.00	-2.00	-3.72	0.83
	SEX_15	18	0.00	0.00	0.00	0.00
	AGE_15	18	-4.44	-2.88	-3.90	0.49
	TMO_15	17	-5.73	-0.06	-2.18	1.42
	TLR_15	17	-6.46	-2.46	-4.65	1.04
	TOC_15	18	-5.35	-1.73	-3.62	1.20
	LOW_15	17	-4.28	0.64	-1.13	1.34
	ROW_15	17	-3.49	0.53	-1.33	1.05
	LOH_15	18	-4.24	3.83	-0.85	2.01
	ROH_15	18	-3.22	2.87	-0.66	1.38
	CASE_06	20	1.00	33.00	15.55	10.48
	TP_06	18	21.00	29.00	23.72	1.74
	SEX_06	18	1.00	2.00	1.44	0.51
	AGE_06	18	9.04	9.94	9.48	0.30
	TMO_06	18	17.65	26.74	22.50	2.20
	TLR_06	18	86.21	94.82	91.03	2.64
	TOC_06	18	55.80	63.12	59.07	2.22
	LOW_06	18	32.13	36.02	34.23	1.23
	ROW_06	18	31.25	36.77	34.30	1.35
	LOH_06	18	35.04	43.89	39.88	2.32

N Obs	Variable	N	Minimum	Maximum	Mean	Std Dev
20	ROH_06	18	37.84	43.43	40.32	1.86
	CASE_16	20	0.00	0.00	0.00	0.00
	TP_16	18	-4.00	5.00	-2.50	1.95
	SEX_16	18	0.00	0.00	0.00	0.00
	AGE_16	18	-3.37	-1.99	-2.94	0.42
	TMO_16	18	-3.02	0.93	-1.57	1.23
	TLR_16	18	-7.15	-0.65	-3.45	1.55
	TOC_16	18	-3.93	-1.05	-2.45	0.75
	LOW_16	18	-3.97	1.58	-0.68	1.25
	ROW_16	18	-3.12	0.38	-1.20	1.08
	LOH_16	18	-3.45	3.88	-1.12	1.66
	ROH_16	18	-2.54	2.54	-0.41	1.54
	CASE_07	20	1.00	33.00	15.55	10.48
	TP_07	20	21.00	26.00	24.15	1.42
	SEX_07	20	1.00	2.00	1.50	0.51
	AGE_07	20	9.97	10.92	10.47	0.31
	TMO_07	20	18.63	25.83	22.36	2.14
	TLR_07	20	80.23	96.40	91.51	3.88
	TOC_07	20	52.01	63.00	59.08	2.71
	LOW_07	20	30.42	36.68	34.32	1.54
	ROW_07	20	31.18	40.39	34.83	1.95
	LOH_07	20	36.40	46.39	40.48	2.38
	ROH_07	20	35.40	44.95	40.43	2.33
	CASE_17	20	0.00	0.00	0.00	0.00
	TP_17	20	-3.00	-1.00	-1.80	0.52
	SEX_17	20	0.00	0.00	0.00	0.00
	AGE_17	20	-2.32	-0.96	-1.94	0.41
	TMO_17	20	-6.68	1.65	-1.47	1.76
	TLR_17	20	-5.76	-0.16	-2.21	1.24
	TOC_17	20	-4.81	0.37	-1.88	1.28
	LOW_17	20	-2.95	1.27	-0.34	1.30
	ROW_17	20	-1.81	4.00	-0.41	1.26
	LOH_17	20	-2.49	4.06	-0.25	1.56
	ROH_17	20	-2.46	2.63	-0.09	1.37
	CASE_08	20	1.00	33.00	15.55	10.48
	TP_08	17	22.00	27.00	25.35	1.50
	SEX_08	17	1.00	2.00	1.47	0.51
	AGE_08	17	10.94	12.00	11.54	0.30
	TMO_08	17	20.18	27.17	23.71	2.05
	TLR_08	17	82.57	98.94	93.36	4.07
	TOC_08	17	53.59	65.71	60.50	2.79
	LOW_08	17	30.54	36.71	34.67	1.51
	ROW_08	17	31.69	37.54	34.98	1.81
	LOH_08	17	37.62	44.93	40.50	2.21
	ROH_08	17	36.61	44.91	40.44	2.20
	CASE_18	20	0.00	0.00	0.00	0.00
	TP_18	17	-1.00	0.00	-0.82	0.39
	SEX_18	17	0.00	0.00	0.00	0.00
	AGE_18	17	-1.45	0.00	-0.86	0.44
	TMO_18	17	-3.45	0.88	-0.54	1.10
	TLR_18	17	-3.71	1.58	-0.85	1.55
	TOC_18	17	-3.63	0.34	-0.79	1.03
	LOW_18	17	-3.34	2.43	-0.00	1.32
	ROW_18	17	-2.26	1.05	-0.31	0.74
	LOH_18	17	-2.63	1.84	-0.32	1.27

N Obs	Variable	N	Minimum	Maximum	Mean	Std Dev
20	ROH_18	17	-2.98	2.39	-0.28	1.36
	CASE_09	20	1.00	33.00	15.55	10.48
	TP_09	16	23.00	28.00	25.94	1.61
	SEX_09	16	1.00	2.00	1.62	0.50
	AGE_09	16	12.02	12.90	12.49	0.28
	TMO_09	16	19.24	29.55	23.58	2.73
	TLR_09	16	83.37	99.50	93.46	4.39
	TOC_09	16	53.25	66.52	60.82	3.25
	LOW_09	16	30.28	39.59	34.66	2.11
	ROW_09	16	31.76	38.70	35.23	1.75
	LOH_09	16	36.23	45.37	40.52	2.86
	ROH_09	16	36.72	45.92	40.51	2.68
	CASE_19	20	0.00	0.00	0.00	0.00
	TP_19	16	0.00	1.00	0.06	0.25
	SEX_19	16	0.00	0.00	0.00	0.00
	AGE_19	16	0.00	0.78	0.05	0.20
	TMO_19	16	-0.88	0.00	-0.05	0.22
	TLR_19	16	-0.08	0.00	-0.01	0.02
	TOC_19	16	0.00	0.47	0.03	0.12
	LOW_19	16	0.00	1.48	0.09	0.37
	ROW_19	16	-0.69	0.00	-0.04	0.17
	LOH_19	16	-0.30	0.00	-0.02	0.08
	ROH_19	16	-0.45	0.00	-0.03	0.11

Table 9. (cont.) Measurements of Interorbital Distances, Orbital Widths and Heights

N Obs	Variable	N	Minimum	Maximum	Mean	Std Dev
20	STUDY_01	20	9505.00	9505.00	9505.00	0.00
	CASE_01	20	1.00	33.00	15.55	10.48
	TP_01	20	23.00	28.00	25.95	1.57
	SEX_01	20	1.00	2.00	1.50	0.51
	AGE_01	20	11.13	13.07	12.41	0.46
	TMO_01	20	19.24	29.55	23.83	2.59
	TLR_01	20	83.37	99.50	93.72	4.02
	TOC_01	20	53.25	66.52	60.95	2.89
	LOW_01	20	30.28	39.59	34.66	1.93
	ROW_01	20	31.76	38.70	35.24	1.62
	LOH_01	20	36.23	45.37	40.73	2.62
	ROH_01	20	36.72	45.92	40.52	2.49
	CASE_0A	20	1.00	33.00	15.55	10.48
	TP_0A	17	24.00	29.00	26.76	1.39
	SEX_0A	17	1.00	2.00	1.47	0.51
	AGE_0A	17	13.01	13.97	13.48	0.33
	TMO_0A	17	20.01	28.62	24.13	2.31
	TLR_0A	17	85.32	99.87	94.38	4.09
	TOC_0A	17	54.98	67.89	61.31	3.22
	LOW_0A	17	32.18	36.80	34.92	1.49
	ROW_0A	17	31.42	38.10	35.33	1.75
	LOH_0A	17	34.15	46.25	41.24	3.02
	ROH_0A	17	33.81	48.17	41.00	3.23
	CASE_1A	20	0.00	0.00	0.00	0.00
	TP_1A	17	0.00	2.00	0.94	0.43
	SEX_1A	17	0.00	0.00	0.00	0.00
	AGE_1A	17	0.00	1.97	1.03	0.46
	TMO_1A	17	-1.22	4.03	0.52	1.28
	TLR_1A	17	-1.48	4.73	1.14	1.41
	TOC_1A	17	-0.64	1.84	0.61	0.83
	LOW_1A	17	-3.10	3.32	0.31	1.48
	ROW_1A	17	-1.11	2.70	0.31	1.01
	LOH_1A	17	-2.08	3.20	0.55	1.37
	ROH_1A	17	-2.91	3.47	0.62	1.39
	CASE_0B	20	1.00	33.00	15.55	10.48
	TP_0B	18	25.00	29.00	27.61	1.46
	SEX_0B	18	1.00	2.00	1.50	0.51
	AGE_0B	18	14.01	14.99	14.45	0.29
	TMO_0B	18	20.63	28.39	24.34	2.29
	TLR_0B	18	86.43	104.22	96.27	4.01
	TOC_0B	18	56.22	67.57	62.07	2.81
	LOW_0B	18	32.07	39.34	35.83	1.53
	ROW_0B	18	31.92	39.40	36.11	2.10
	LOH_0B	18	34.06	44.37	41.32	2.66
	ROH_0B	18	35.14	43.63	40.19	2.28
	CASE_1B	20	0.00	0.00	0.00	0.00
	TP_1B	18	1.00	3.00	1.78	0.55
	SEX_1B	18	0.00	0.00	0.00	0.00
	AGE_1B	18	1.00	3.35	2.10	0.58
	TMO_1B	18	-2.03	6.58	0.78	1.89
	TLR_1B	18	0.31	5.71	2.62	1.61
	TOC_1B	18	-1.09	3.40	1.39	1.37
	LOW_1B	18	-2.27	3.80	1.05	1.35
	ROW_1B	18	-0.05	3.01	0.79	0.86
	LOH_1B	18	-4.09	5.54	0.82	2.22

TP 01: Reference Age 12.   TP A-G: Age 13-19

N Obs	Variable	N	Minimum	Maximum	Mean	Std Dev
20	ROH_1B	18	-7.58	4.33	-0.13	2.92
	CASE_0C	20	1.00	33.00	15.55	10.48
	TP_0C	18	26.00	30.00	28.72	1.27
	SEX_0C	18	1.00	2.00	1.50	0.51
	AGE_0C	18	15.08	16.51	15.56	0.36
	TMO_0C	18	19.11	28.77	24.30	2.47
	TLR_0C	18	89.83	103.14	96.50	3.91
	TOC_0C	18	57.63	68.90	62.27	3.05
	LOW_0C	18	33.43	38.34	36.01	1.26
	ROW_0C	18	34.36	38.76	36.20	1.23
	LOH_0C	18	37.57	46.85	42.17	2.77
	ROH_0C	18	38.11	47.28	41.36	2.37
	CASE_1C	20	0.00	0.00	0.00	0.00
	TP_1C	18	2.00	5.00	2.94	0.73
	SEX_1C	18	0.00	0.00	0.00	0.00
	AGE_1C	18	2.09	4.38	3.18	0.71
	TMO_1C	18	-1.68	2.80	0.44	0.97
	TLR_1C	18	-0.20	6.82	3.30	2.18
	TOC_1C	18	-0.63	4.37	1.66	1.48
	LOW_1C	18	-0.52	4.45	1.65	1.36
	ROW_1C	18	-0.10	3.12	1.22	0.91
	LOH_1C	18	-1.41	6.79	1.70	2.04
	ROH_1C	18	-1.06	4.57	1.03	1.66
	CASE_0D	20	1.00	33.00	15.55	10.48
	TP_0D	8	27.00	31.00	29.62	1.51
	SEX_0D	8	1.00	2.00	1.37	0.52
	AGE_0D	8	16.10	17.50	16.60	0.45
	TMO_0D	8	21.53	29.52	25.62	3.08
	TLR_0D	8	90.19	103.61	97.47	5.68
	TOC_0D	8	58.37	67.58	63.58	4.12
	LOW_0D	8	33.18	38.04	35.73	1.57
	ROW_0D	8	33.54	39.03	36.12	2.06
	LOH_0D	8	38.76	46.13	42.42	2.63
	ROH_0D	8	37.50	48.72	42.13	3.66
	CASE_1D	20	0.00	0.00	0.00	0.00
	TP_1D	8	3.00	5.00	3.87	0.64
	SEX_1D	8	0.00	0.00	0.00	0.00
	AGE_1D	8	3.29	5.49	4.07	0.72
	TMO_1D	8	-1.31	5.17	1.60	2.07
	TLR_1D	8	1.11	7.87	4.57	2.37
	TOC_1D	8	-1.10	6.99	2.91	2.43
	LOW_1D	8	-1.55	3.85	1.62	1.72
	ROW_1D	8	-1.01	4.04	1.34	1.54
	LOH_1D	8	-0.58	4.52	1.65	1.52
	ROH_1D	8	-0.36	3.13	1.02	1.27
	CASE_0E	20	1.00	33.00	15.55	10.48
	TP_0E	4	28.00	32.00	30.25	1.71
	SEX_0E	4	1.00	2.00	1.50	0.58
	AGE_0E	4	17.51	17.92	17.71	0.17
	TMO_0E	4	23.01	28.05	24.94	2.40
	TLR_0E	4	91.74	104.81	97.90	6.37
	TOC_0E	4	59.41	65.09	62.09	2.59
	LOW_0E	4	33.78	41.29	36.70	3.39
	ROW_0E	4	33.15	40.42	36.27	3.10
	LOH_0E	4	39.74	43.14	41.13	1.44

N Obs	Variable	N	Minimum	Maximum	Mean	Std Dev
20	ROH_0E	4	38.86	42.39	40.79	1.46
	CASE_1E	20	0.00	0.00	0.00	0.00
	TP_1E	4	4.00	5.00	4.75	0.50
	SEX_1E	4	0.00	0.00	0.00	0.00
	AGE_1E	4	4.81	6.38	5.53	0.66
	TMO_1E	4	-2.30	1.80	0.18	1.84
	TLR_1E	4	1.85	7.73	5.53	2.73
	TOC_1E	4	-0.80	4.50	1.87	2.20
	LOW_1E	4	0.98	5.75	3.25	2.03
	ROW_1E	4	0.81	4.03	2.10	1.52
	LOH_1E	4	-0.49	4.64	1.85	2.26
	ROH_1E	4	0.09	4.09	1.40	1.82
	CASE_0F	20	1.00	33.00	15.55	10.48
	TP_0F	1	28.00	28.00	28.00	.
	SEX_0F	1	2.00	2.00	2.00	.
	AGE_0F	1	18.46	18.46	18.46	.
	TMO_0F	1	24.39	24.39	24.39	.
	TLR_0F	1	91.63	91.63	91.63	.
	TOC_0F	1	59.51	59.51	59.51	.
	LOW_0F	1	33.46	33.46	33.46	.
	ROW_0F	1	33.77	33.77	33.77	.
	LOH_0F	1	37.41	37.41	37.41	.
	ROH_0F	1	37.20	37.20	37.20	.
	CASE_1F	20	0.00	0.00	0.00	0.00
	TP_1F	1	5.00	5.00	5.00	.
	SEX_1F	1	0.00	0.00	0.00	.
	AGE_1F	1	5.90	5.90	5.90	.
	TMO_1F	1	3.06	3.06	3.06	.
	TLR_1F	1	8.26	8.26	8.26	.
	TOC_1F	1	6.26	6.26	6.26	.
	LOW_1F	1	3.19	3.19	3.19	.
	ROW_1F	1	2.01	2.01	2.01	.
	LOH_1F	1	1.07	1.07	1.07	.
	ROH_1F	1	-0.66	-0.66	-0.66	.
	CASE_0G	20	1.00	33.00	15.55	10.48
	TP_0G	1	31.00	31.00	31.00	.
	SEX_0G	1	1.00	1.00	1.00	.
	AGE_0G	1	19.01	19.01	19.01	.
	TMO_0G	1	28.63	28.63	28.63	.
	TLR_0G	0	.	.	.	.
	TOC_0G	1	66.09	66.09	66.09	.
	LOW_0G	1	36.27	36.27	36.27	.
	ROW_0G	0	.	.	.	.
	LOH_0G	1	40.64	40.64	40.64	.
	ROH_0G	1	40.89	40.89	40.89	.
	CASE_1G	20	0.00	0.00	0.00	0.00
	TP_1G	1	6.00	6.00	6.00	.
	SEX_1G	1	0.00	0.00	0.00	.
	AGE_1G	1	6.73	6.73	6.73	.
	TMO_1G	1	1.88	1.88	1.88	.
	LR_1G	0	.	.	.	.
	TOC_1G	1	5.49	5.49	5.49	.
	LOW_1G	1	2.93	2.93	2.93	.
	ROW_1G	0	.	.	.	.
	LOH_1G	1	2.49	2.49	2.49	.

Table 10. Measurements of Upper, Lower Orbital Heights and Upper orbital Height Ratio•

N Obs	Variable	N	Minimum	Maximum	Mean	Std Dev
20	CASE_01	20	1.00	33.00	15.55	10.48
	LUP_02	2	14.48	15.77	15.13	0.91
	LUP_03	7	12.01	17.83	15.51	2.09
	LUP_04	14	11.07	17.27	14.95	1.86
	LUP_05	18	9.71	17.40	15.07	2.17
	LUP_06	18	11.43	19.09	14.98	1.74
	LUP_07	20	10.58	18.08	15.06	1.96
	LUP_08	17	10.47	18.36	14.95	2.11
	LUP_09	16	10.79	17.56	14.11	1.76
	LLOW_01	19	22.27	32.54	26.26	2.83
	LLOW_02	2	21.86	27.70	24.78	4.13
	LLOW_03	7	20.26	27.54	24.12	2.78
	LLOW_04	14	21.09	30.18	25.43	3.05
	LLOW_05	18	21.76	31.07	24.91	2.50
	LLOW_06	18	20.38	28.87	24.85	2.44
	LLOW_07	20	21.99	32.66	25.34	2.77
	LLOW_08	17	22.46	30.11	25.48	2.52
	LLOW_09	16	22.27	33.38	26.35	3.18
	RUP_01	19	7.33	18.10	13.59	2.24
	RUP_02	2	14.90	17.36	16.13	1.74
	RUP_03	7	12.98	16.96	15.03	1.50
	RUP_04	14	0.95	17.06	13.61	4.16
	RUP_05	18	7.51	18.23	14.78	2.42
	RUP_06	18	9.07	18.27	14.34	2.34
	RUP_07	20	8.53	17.70	14.23	2.10
	RUP_08	17	9.10	18.10	14.37	2.08
	RUP_09	16	9.40	16.33	13.48	1.77
	RLOW_01	19	22.99	32.33	26.63	2.70
	RLOW_02	2	22.91	26.97	24.94	2.87
	RLOW_03	7	21.62	28.30	24.90	2.06
	RLOW_04	14	22.07	30.15	25.62	2.61
	RLOW_05	18	21.70	30.09	25.05	2.22
	RLOW_06	18	22.45	29.98	25.83	2.24
	RLOW_07	20	22.24	32.29	26.06	2.69
	RLOW_08	17	23.21	30.83	25.90	2.42
	RLOW_09	16	22.99	34.51	26.92	3.13
	PRUL_02	2	34.33	41.91	38.12	5.36
	PRUL_03	7	30.99	46.61	39.22	5.69
	PRUL_04	14	27.32	43.80	37.17	5.48
	PRUL_05	18	23.81	43.33	37.71	5.27
	PRUL_06	18	28.36	44.81	37.66	4.20
	PRUL_07	20	26.50	44.20	37.35	4.83
	PRUL_08	17	26.19	44.69	37.00	4.86
	PRUL_09	16	25.34	41.23	35.00	4.61
	PRUR_02	2	35.59	43.11	39.35	5.32
	PRUR_03	7	31.44	42.21	37.69	3.92
	PRUR_04	14	3.19	42.26	34.13	10.25
	PRUR_05	18	19.97	43.78	37.06	5.59
	PRUR_06	18	23.38	43.28	35.66	5.32
	PRUR_07	20	22.42	44.32	35.36	5.11
	PRUR_08	17	23.59	43.67	35.69	4.80
	PRUR_09	16	21.41	39.20	33.48	4.64
	PRUAV_02	2	34.96	42.51	38.73	5.34
	PRUAV_03	7	31.21	44.32	38.45	4.76
	PRUAV_04	14	16.49	42.79	35.65	7.41

TP 01: Reference Age 12. TP 02-09: Age 5-12.

N Obs	Variable	N	Minimum	Maximum	Mean	Std Dev
20	PRUAV_05	18	21.89	43.17	37.38	5.35
	PRUAV_06	18	25.87	44.05	36.66	4.65
	PRUAV_07	20	24.46	42.96	36.35	4.85
	PRUAV_08	17	24.89	43.45	36.34	4.75
	PRUAV_09	16	23.37	40.21	34.24	4.55

PRUL: left upper orbital height ratio
PRUR: right upper orbital height ratio
PRUAV: average of right and left upper orbital height ratio

Table 10. (cont.) Measurements of Upper, Lower Orbital Heights and Upper Orbital Height Ratio

N Obs	Variable	N	Minimum	Maximum	Mean	Std Dev
20	CASE_01	20	1.00	33.00	15.55	10.48
	LUP_0A	17	9.32	17.06	14.11	2.23
	LUP_0B	18	10.71	18.55	14.91	2.11
	LUP_0C	18	10.52	18.14	15.45	2.02
	LUP_0D	8	12.93	16.26	15.17	1.15
	LUP_0E	4	14.58	17.12	15.53	1.10
	LUP_0F	1	11.63	11.63	11.63	.
	LUP_0G	1	14.82	14.82	14.82	.
	LLOW_0A	17	21.12	32.54	27.04	3.42
	LLOW_0B	18	20.21	31.57	26.29	2.83
	LLOW_0C	18	22.82	31.45	26.65	2.39
	LLOW_0D	8	25.03	31.48	27.15	2.51
	LLOW_0E	4	25.11	26.02	25.54	0.39
	LLOW_0F	1	25.76	25.76	25.76	.
	LLOW_0G	2	0.00	25.77	12.89	18.22
	RUP_0A	17	0.00	17.07	12.49	4.04
	RUP_0B	18	9.67	17.71	14.16	2.06
	RUP_0C	18	7.72	17.87	14.55	2.39
	RUP_0D	8	11.75	16.69	14.51	1.62
	RUP_0E	4	13.94	16.01	15.05	0.89
	RUP_0F	1	10.45	10.45	10.45	.
	RUP_0G	1	14.77	14.77	14.77	.
	RLOW_0A	17	22.05	33.22	27.53	3.55
	RLOW_0B	18	20.00	30.92	25.87	2.76
	RLOW_0C	18	23.40	31.35	26.68	2.42
	RLOW_0D	8	24.18	32.18	27.51	3.37
	RLOW_0E	4	23.92	26.82	25.52	1.33
	RLOW_0F	1	26.61	26.61	26.61	.
	RLOW_0G	1	26.00	26.00	26.00	.
	PRUL_0A	17	22.26	43.89	34.39	5.55
	PRUL_0B	18	25.51	42.41	36.24	4.84
	PRUL_0C	18	26.01	40.99	36.68	4.06
	PRUL_0D	8	30.86	38.67	35.92	2.82
	PRUL_0E	4	36.73	39.68	37.78	1.31
	PRUL_0F	1	31.10	31.10	31.10	.
	PRUL_0G	1	36.51	36.51	36.51	.
	PRUR_0A	17	18.48	41.04	32.80	5.96
	PRUR_0B	18	24.60	43.19	35.43	5.24
	PRUR_0C	18	19.76	42.46	35.26	5.25
	PRUR_0D	8	28.77	39.01	34.64	3.86
	PRUR_0E	4	34.57	39.08	37.11	1.98
	PRUR_0F	1	28.20	28.20	28.20	.
	PRUR_0G	1	36.23	36.23	36.23	.
	PRUAV_0A	17	20.37	42.37	33.59	5.70
	PRUAV_0B	18	25.06	42.60	35.84	4.99
	PRUAV_0C	18	22.89	41.72	35.97	4.52
	PRUAV_0D	8	29.82	38.80	35.28	3.32
	PRUAV_0E	4	35.88	38.30	37.45	1.10
	PRUAV_0F	1	29.65	29.65	29.65	.
	PRUAV_0G	1	36.37	36.37	36.37	.

TP 01: Reference Age 12. TP 0A-0G: Age 13-19
PRUL: left upper orbital height ratio
PRUR: right upper orbital height ratio
PRUAV: average of right and left upper orbital height ratio

Table 11. Measurements of Horizontal and Vertical Displacement of Gravity Center of Maxillary Implants Relative to Reference Lines

N Obs	Variable	N	Minimum	Maximum	Mean	Std Dev
10	CASE_01	10	4.00	33.00	21.80	10.13
	TP_01	10	23.00	28.00	26.30	1.49
	SEX_01	10	1.00	2.00	1.50	0.53
	AGE_01	10	11.89	13.07	12.50	0.40
	CG2AX_01	9	-1.75	0.84	-0.39	0.82
	CG2AY_01	9	5.52	11.18	8.71	1.66
	IMPAX_01	8	-7.84	2.89	-1.27	3.94
	IMPAY_01	8	-45.35	-34.33	-39.40	3.74
	CG2BX_01	9	-1.74	0.90	-0.30	0.83
	CG2BY_01	9	-4.13	1.80	-1.23	2.11
	IMPBX_01	8	-7.79	4.54	-0.93	4.12
	IMPBY_01	8	-53.87	-42.34	-49.63	3.89
	CG2CX_01	9	-1.83	0.73	-0.39	0.83
	CG2CY_01	9	4.44	14.54	10.25	3.29
	IMPCX_01	8	-8.25	2.30	-1.51	3.84
	IMPCY_01	8	-43.18	-32.97	-37.72	3.37
	CG2DX_01	9	-1.83	0.99	-0.28	0.88
	CG2DY_01	9	-10.70	-6.30	-8.50	1.66
	IMPDX_01	8	-8.24	4.03	-0.84	4.25
	IMPDY_01	8	-62.85	-51.37	-56.75	4.01
	CG2EX_01	9	-1.65	0.91	-0.27	0.82
	CG2EY_01	9	-1.10	4.05	1.13	1.65
	IMPEX_01	8	-7.31	4.76	-0.80	4.16
	IMPEY_01	8	-50.39	-41.10	-47.25	3.36
	CG2FX_01	9	-1.98	1.05	-0.32	0.91
	CG2FY_01	9	-7.84	1.03	-4.04	2.94
	IMPFX_01	8	-9.00	3.06	-1.07	4.58
	IMPFY_01	8	-59.45	-47.24	-52.68	4.60
	AGE_12	0	.	.	.	.
	CG2AX_12	0	.	.	.	.
	CG2AY_12	0	.	.	.	.
	IMPAX_12	0	.	.	.	.
	IMPAY_12	0	.	.	.	.
	CG2BX_12	0	.	.	.	.
	CG2BY_12	0	.	.	.	.
	IMPBX_12	0	.	.	.	.
	IMPBY_12	0	.	.	.	.
	CG2CX_12	0	.	.	.	.
	CG2CY_12	0	.	.	.	.
	IMPCX_12	0	.	.	.	.
	IMPCY_12	0	.	.	.	.
	CG2DX_12	0	.	.	.	.
	CG2DY_12	0	.	.	.	.
	IMPDX_12	0	.	.	.	.
	IMPDY_12	0	.	.	.	.
	CG2EX_12	0	.	.	.	.
	CG2EY_12	0	.	.	.	.
	IMPEX_12	0	.	.	.	.
	IMPEY_12	0	.	.	.	.
	CG2FX_12	0	.	.	.	.
	CG2FY_12	0	.	.	.	.
	IMPFX_12	0	.	.	.	.
	IMPFY_12	0	.	.	.	.
	AGE_13	4	-6.31	-4.93	-5.74	0.58
	CG2AX_13	4	-0.62	6.32	1.41	3.30

TP 01: Reference Age 12.   TP 02-09: Age 5-12.

N Obs	Variable	N	Minimum	Maximum	Mean	Std Dev
10	CG2AY_13	4	-0.75	4.15	0.55	2.40
	IMPAX_13	3	0.05	0.32	0.18	0.14
	IMPAY_13	3	1.53	3.24	2.41	0.86
	CG2BX_13	4	-0.54	6.87	1.56	3.55
	CG2BY_13	4	-0.79	4.50	1.63	2.40
	IMPBX_13	3	-0.21	1.16	0.67	0.76
	IMPBY_13	3	1.24	6.35	3.66	2.57
	CG2CX_13	4	-3.20	1.83	-1.21	2.27
	CG2CY_13	4	2.84	8.28	4.81	2.57
	IMPCX_13	3	-2.47	-1.87	-2.26	0.34
	IMPCY_13	3	6.57	11.47	8.45	2.64
	CG2DX_13	4	-0.77	6.28	1.50	3.24
	CG2DY_13	4	-0.72	5.26	1.82	2.52
	IMPDX_13	3	0.01	0.73	0.32	0.37
	IMPDY_13	3	2.48	4.74	3.67	1.13
	CG2EX_13	4	-0.97	6.24	1.27	3.35
	CG2EY_13	4	-0.97	4.10	1.46	2.34
	IMPEX_13	3	0.55	0.93	0.80	0.22
	IMPEY_13	3	1.08	6.32	3.55	2.63
	CG2FX_13	4	-0.76	6.62	1.31	3.55
	CG2FY_13	4	-0.23	4.01	2.10	1.79
	IMPFX_13	3	-0.93	0.20	-0.19	0.64
	IMPFY_13	3	2.97	5.57	4.44	1.33
	AGE_14	7	-5.66	-4.03	-4.94	0.51
	CG2AX_14	5	-7.37	1.89	-1.23	3.57
	CG2AY_14	5	-8.55	1.37	-1.73	4.01
	IMPAX_14	4	-0.82	2.25	0.36	1.42
	IMPAY_14	4	3.07	6.49	4.10	1.62
	CG2BX_14	5	-6.77	1.14	-1.34	3.14
	CG2BY_14	5	-7.59	2.16	-0.93	3.89
	IMPBX_14	4	-1.40	1.08	0.14	1.07
	IMPBY_14	4	1.76	6.58	4.84	2.27
	CG2CX_14	3	-0.34	4.91	1.58	2.89
	CG2CY_14	3	-1.31	4.83	1.95	3.09
	IMPCX_14	3	-2.81	4.80	0.43	3.93
	IMPCY_14	3	3.81	6.89	5.86	1.78
	CG2DX_14	5	-7.17	1.71	-1.25	3.46
	CG2DY_14	5	-7.83	1.49	-1.29	3.80
	IMPDX_14	4	-0.37	0.99	0.38	0.56
	IMPDY_14	4	3.50	6.08	4.46	1.17
	CG2EX_14	5	-7.38	1.34	-1.37	3.47
	CG2EY_14	5	-8.07	1.18	-1.88	3.57
	IMPEX_14	4	-0.17	1.33	0.72	0.65
	IMPEY_14	4	0.91	5.49	3.77	1.98
	CG2FX_14	5	-6.72	1.53	-1.31	3.20
	CG2FY_14	5	-7.78	2.28	-0.67	4.18
	IMPFX_14	4	-0.72	0.93	0.03	0.68
	IMPFY_14	4	3.98	7.39	5.22	1.58
	AGE_15	9	-4.44	-2.90	-3.90	0.49
	CG2AX_15	8	-1.64	1.81	-0.20	1.19
	CG2AY_15	8	-4.82	0.49	-1.31	1.81
	IMPAX_15	7	-0.68	2.08	0.11	0.94
	IMPAY_15	7	0.00	4.25	2.19	1.56
	CG2BX_15	8	-1.37	1.43	-0.23	0.97
	CG2BY_15	8	-1.71	2.57	-0.36	1.29

N Obs	Variable	N	Minimum	Maximum	Mean	Std Dev
10	IMPBX_15	7	-0.81	1.37	0.20	0.68
	IMPBY_15	7	-0.39	5.16	3.32	1.75
	CG2CX_15	7	-4.25	3.56	-0.96	2.58
	CG2CY_15	7	-0.74	4.84	1.98	1.90
	IMPCX_15	6	-4.90	2.60	-0.68	2.68
	IMPCY_15	6	4.57	8.09	6.04	1.34
	CG2DX_15	8	-1.63	1.99	-0.18	1.24
	CG2DY_15	8	-2.64	2.11	-0.67	1.61
	IMPDX_15	7	-0.60	0.63	-0.07	0.50
	IMPDY_15	7	2.18	4.54	2.98	0.92
	CG2EX_15	8	-1.44	1.72	0.01	1.04
	CG2EY_15	8	-2.71	1.77	-0.92	1.40
	IMPEX_15	7	-0.93	1.48	0.57	0.89
	IMPEY_15	7	-0.33	4.27	2.82	1.58
	CG2FX_15	8	-1.51	1.37	-0.23	0.92
	CG2FY_15	8	-2.28	2.78	-0.15	1.83
	IMPFX_15	7	-0.88	0.54	-0.11	0.43
	IMPFY_15	7	2.09	5.52	3.66	1.26
	AGE_16	9	-3.37	-1.99	-2.89	0.48
	CG2AX_16	8	-0.71	2.29	0.18	0.99
	CG2AY_16	8	-4.10	0.05	-1.67	1.57
	IMPAX_16	7	-1.18	1.87	0.19	1.21
	IMPAY_16	7	-0.35	3.11	1.50	1.20
	CG2BX_16	8	-1.82	1.66	-0.16	1.03
	CG2BY_16	8	-2.38	1.91	-0.42	1.33
	IMPBX_16	7	-0.44	0.72	0.14	0.47
	IMPBY_16	7	1.78	5.00	2.98	1.11
	CG2CX_16	7	-2.94	0.28	-1.30	0.99
	CG2CY_16	7	-3.07	4.63	0.71	2.59
	IMPCX_16	6	-1.75	0.17	-1.10	0.71
	IMPCY_16	6	1.68	6.01	4.06	1.61
	CG2DX_16	8	-1.43	1.96	-0.11	1.09
	CG2DY_16	8	-3.30	0.30	-1.11	1.27
	IMPDX_16	7	-0.50	1.06	0.16	0.49
	IMPDY_16	7	0.32	3.83	2.14	1.23
	CG2EX_16	8	-1.29	2.09	0.00	1.05
	CG2EY_16	8	-2.54	1.50	-0.76	1.44
	IMPEX_16	7	-0.26	1.43	0.44	0.62
	IMPEY_16	7	1.71	4.53	2.61	1.08
	CG2FX_16	8	-1.42	1.87	-0.31	1.00
	CG2FY_16	8	-3.11	0.96	-0.82	1.44
	IMPFX_16	7	-0.63	1.36	-0.09	0.66
	IMPFY_16	7	1.02	4.18	2.57	1.23
	AGE_17	10	-2.32	-0.96	-1.89	0.46
	CG2AX_17	9	-0.99	1.70	0.23	1.13
	CG2AY_17	9	-3.64	1.57	-1.00	2.05
	IMPAX_17	8	-1.55	2.57	0.02	1.44
	IMPAY_17	8	-1.10	1.87	0.78	0.90
	CG2BX_17	9	-0.38	1.15	0.14	0.59
	CG2BY_17	9	-3.22	3.62	-0.33	1.91
	IMPBX_17	8	-0.71	1.67	0.43	0.69
	IMPBY_17	8	-1.08	4.10	1.53	1.67
	CG2CX_17	9	-5.19	1.91	-0.59	2.10
	CG2CY_17	9	-2.91	10.15	1.90	4.34
	IMPCX_17	8	-6.14	1.34	-0.95	2.44

N Obs	Variable	N	Minimum	Maximum	Mean	Std Dev
10	IMPCY_17	8	-2.45	10.15	3.50	4.04
	CG2DX_17	9	-0.62	2.28	0.26	0.99
	CG2DY_17	9	-2.29	1.74	-0.44	1.48
	IMPDX_17	8	-0.58	2.69	0.45	1.02
	IMPDY_17	8	0.06	2.21	1.24	0.79
	CG2EX_17	9	-0.67	1.53	0.14	0.83
	CG2EY_17	9	-3.39	2.28	-1.04	1.86
	IMPEX_17	8	-0.19	2.04	0.65	0.80
	IMPEY_17	8	-1.65	2.65	0.75	1.64
	CG2FX_17	9	-1.01	1.23	-0.01	0.81
	CG2FY_17	9	-3.79	2.39	-0.28	2.05
	IMPFX_17	8	-0.69	1.44	0.24	0.69
	IMPFY_17	8	0.12	2.84	1.63	0.95
	AGE_18	10	-1.45	0.00	-0.82	0.47
	CG2AX_18	9	-0.14	0.75	0.09	0.30
	CG2AY_18	9	-4.36	1.14	-0.78	1.68
	IMPAX_18	8	-0.91	1.33	0.41	0.78
	IMPAY_18	8	-0.47	1.08	0.28	0.55
	CG2BX_18	9	-0.42	0.95	0.05	0.40
	CG2BY_18	9	-2.92	1.24	-0.63	1.48
	IMPBX_18	8	-0.71	1.10	0.30	0.57
	IMPBY_18	8	-1.12	1.99	0.47	1.13
	CG2CX_18	9	-2.75	1.08	-0.55	1.27
	CG2CY_18	9	-2.99	5.81	0.89	2.77
	IMPCX_18	8	-4.26	1.45	-0.53	2.02
	IMPCY_18	8	-0.34	6.04	1.80	2.35
	CG2DX_18	9	-0.73	0.62	-0.00	0.35
	CG2DY_18	9	-3.08	0.46	-0.67	1.22
	IMPDX_18	8	-0.37	1.53	0.18	0.59
	IMPDY_18	8	-0.57	1.30	0.37	0.70
	CG2EX_18	9	-0.69	0.47	-0.02	0.41
	CG2EY_18	9	-3.27	0.90	-0.91	1.60
	IMPEX_18	8	-0.51	1.58	0.31	0.70
	IMPEY_18	8	-1.51	1.62	0.20	0.99
	CG2FX_18	9	-1.15	0.38	-0.19	0.48
	CG2FY_18	9	-3.27	0.90	-0.68	1.48
	IMPFX_18	8	-0.81	1.11	-0.14	0.60
	IMPFY_18	8	-1.39	1.72	0.47	1.02
	AGE_19	7	0.00	0.78	0.11	0.29
	CG2AX_19	7	-0.18	0.00	-0.03	0.07
	CG2AY_19	7	0.00	0.59	0.08	0.22
	IMPAX_19	6	0.00	0.15	0.02	0.06
	IMPAY_19	6	-0.92	0.00	-0.15	0.38
	CG2BX_19	7	-0.70	0.00	-0.10	0.26
	CG2BY_19	7	-3.59	0.00	-0.51	1.36
	IMPBX_19	6	0.00	1.05	0.18	0.43
	IMPBY_19	6	-5.02	0.00	-0.84	2.05
	CG2CX_19	7	0.00	0.64	0.09	0.24
	CG2CY_19	7	0.00	2.32	0.33	0.88
	IMPCX_19	6	0.00	0.19	0.03	0.08
	IMPCY_19	6	0.00	0.78	0.13	0.32
	CG2DX_19	7	-0.45	0.00	-0.06	0.17
	CG2DY_19	7	0.00	0.49	0.07	0.19
	IMPDX_19	6	0.00	0.13	0.02	0.05
	IMPDY_19	6	-1.01	0.00	-0.17	0.41

N Obs	Variable	N	Minimum	Maximum	Mean	Std Dev
10	CG2EX_19	7	-0.46	0.00	-0.07	0.17
	CG2EY_19	7	-3.38	0.00	-0.48	1.28
	IMPEX_19	6	0.00	1.05	0.18	0.43
	IMPEY_19	6	-4.83	0.00	-0.81	1.97
	CG2FX_19	7	-0.41	0.00	-0.06	0.15
	CG2FY_19	7	0.00	0.95	0.14	0.36
	IMPFX_19	6	-0.32	0.00	-0.05	0.13
	IMPFY_19	6	-0.57	0.00	-0.09	0.23

CG: crista galli
IMP: gravity center of maxillary implants
X: horizontal measurements
y: vertical measurements
A: reference line #6 (see Figure 7)
B: reference line #4 (see Figure 7)
C: reference line #1 (see Figure 7)
D: reference line #2 (see Figure 7)
E: reference line #5 (see Figure 7)
F: reference line #3 (see Figure 7)

Table 11 (cont.). Measurements of Horizontal and Vertical Displacement of Gravity Center of Maxillary Implants Relative to Reference Lines

N Obs	Variable	N	Minimum	Maximum	Mean	Std Dev
10	CASE_01	10	4.00	33.00	21.80	10.13
	TP_01	10	23.00	28.00	26.30	1.49
	SEX_01	10	1.00	2.00	1.50	0.53
	AGE_01	10	11.89	13.07	12.50	0.40
	CG2AX_01	9	-1.75	0.84	-0.39	0.82
	CG2AY_01	9	5.52	11.18	8.71	1.66
	IMPAX_01	8	-7.84	2.89	-1.27	3.94
	IMPAY_01	8	-45.35	-34.33	-39.40	3.74
	CG2BX_01	9	-1.74	0.90	-0.30	0.83
	CG2BY_01	9	-4.13	1.80	-1.23	2.11
	IMPBX_01	8	-7.79	4.54	-0.93	4.12
	IMPBY_01	8	-53.87	-42.34	-49.63	3.89
	CG2CX_01	9	-1.83	0.73	-0.39	0.83
	CG2CY_01	9	4.44	14.54	10.25	3.29
	IMPCX_01	8	-8.25	2.30	-1.51	3.84
	IMPCY_01	8	-43.18	-32.97	-37.72	3.37
	CG2DX_01	9	-1.83	0.99	-0.28	0.88
	CG2DY_01	9	-10.70	-6.30	-8.50	1.66
	IMPDX_01	8	-8.24	4.03	-0.84	4.25
	IMPDY_01	8	-62.85	-51.37	-56.75	4.01
	CG2EX_01	9	-1.65	0.91	-0.27	0.82
	CG2EY_01	9	-1.10	4.05	1.13	1.65
	IMPEX_01	8	-7.31	4.76	-0.80	4.16
	IMPEY_01	8	-50.39	-41.10	-47.25	3.36
	CG2FX_01	9	-1.98	1.05	-0.32	0.91
	CG2FY_01	9	-7.84	1.03	-4.04	2.94
	IMPFX_01	8	-9.00	3.06	-1.07	4.58
	IMPFY_01	8	-59.45	-47.24	-52.68	4.60
	AGE_1A	9	0.00	1.97	0.94	0.62
	CG2AX_1A	8	-1.19	1.70	0.08	0.95
	CG2AY_1A	8	-2.82	3.04	-0.15	1.89
	IMPAX_1A	6	-1.29	0.90	-0.26	0.72
	IMPAY_1A	6	-1.76	0.21	-0.70	0.92
	CG2BX_1A	8	-1.21	1.10	-0.24	0.74
	CG2BY_1A	8	-2.03	3.46	-0.14	1.66
	IMPBX_1A	6	-0.48	0.94	0.03	0.51
	IMPBY_1A	6	-3.89	0.87	-0.72	1.80
	CG2CX_1A	8	-0.51	4.77	0.97	1.63
	CG2CY_1A	8	-3.05	4.30	0.47	2.13
	IMPCX_1A	6	-0.28	1.63	0.55	0.77
	IMPCY_1A	6	-3.26	3.91	-0.56	2.57
	CG2DX_1A	8	-1.19	1.56	-0.02	0.94
	CG2DY_1A	8	-2.53	3.27	-0.17	1.71
	IMPDX_1A	6	-0.66	1.32	0.10	0.71
	IMPDY_1A	6	-2.24	0.44	-0.74	1.01
	CG2EX_1A	8	-0.99	1.48	-0.09	0.83
	CG2EY_1A	8	-2.59	2.87	-0.69	1.66
	IMPEX_1A	6	-0.17	1.42	0.38	0.59
	IMPEY_1A	6	-4.23	0.13	-1.18	1.75
	CG2FX_1A	8	-1.18	1.19	-0.16	0.77
	CG2FY_1A	8	-2.78	2.43	-0.26	1.62
	IMPFX_1A	6	-0.49	0.56	0.06	0.39
	IMPFY_1A	6	-2.16	0.00	-0.88	0.95
	AGE_1B	10	1.00	2.99	1.98	0.65
	CG2AX_1B	8	-1.72	2.45	0.35	1.59

TP 01: Reference Age 12. TP 0A-0G: Age 13-19.

N Obs	Variable	N	Minimum	Maximum	Mean	Std Dev
10	CG2AY_1B	8	-1.52	2.35	0.37	1.42
	IMPAX_1B	6	-0.69	1.15	0.31	0.73
	IMPAY_1B	6	-2.80	0.74	-0.97	1.34
	CG2BX_1B	8	-1.51	1.61	0.09	1.08
	CG2BY_1B	8	-4.69	3.69	-0.51	2.48
	IMPBX_1B	6	-0.77	2.12	0.51	0.97
	IMPBY_1B	6	-8.72	0.83	-1.76	3.52
	CG2CX_1B	8	-0.38	4.57	1.01	1.62
	CG2CY_1B	8	-6.77	4.18	-1.24	3.24
	IMPCX_1B	6	-2.76	1.68	0.39	1.65
	IMPCY_1B	6	-4.49	0.64	-1.56	1.88
	CG2DX_1B	8	-1.57	1.82	0.01	1.23
	CG2DY_1B	8	-1.82	1.82	0.05	1.05
	IMPDX_1B	6	-1.56	0.80	-0.45	0.85
	IMPDY_1B	6	-3.78	-0.22	-1.13	1.33
	CG2EX_1B	8	-1.40	1.95	0.08	1.21
	CG2EY_1B	8	-3.25	2.51	-0.45	1.95
	IMPEX_1B	6	-0.92	2.07	0.48	1.03
	IMPEY_1B	6	-7.30	0.76	-1.47	2.94
	CG2FX_1B	8	-1.51	1.46	-0.01	0.99
	CG2FY_1B	8	-3.02	1.04	-0.06	1.32
	IMPFX_1B	6	-0.91	0.53	-0.43	0.50
	IMPFY_1B	6	-3.11	-0.30	-1.11	1.13
	AGE_1C	10	2.09	4.15	3.06	0.68
	CG2AX_1C	8	-0.70	1.76	0.22	0.90
	CG2AY_1C	8	-3.66	2.94	-0.28	2.13
	IMPAX_1C	5	-0.57	0.74	0.10	0.61
	IMPAY_1C	5	-3.29	0.25	-1.65	1.55
	CG2BX_1C	8	-1.23	1.15	-0.18	0.91
	CG2BY_1C	8	-3.05	3.31	-1.01	2.15
	IMPBX_1C	5	-0.37	1.14	0.29	0.77
	IMPBY_1C	5	-5.05	0.65	-2.12	2.04
	CG2CX_1C	8	-2.19	3.05	0.33	1.71
	CG2CY_1C	8	-2.76	2.84	-0.48	2.22
	IMPCX_1C	5	-0.86	1.14	0.37	0.75
	IMPCY_1C	5	-3.97	3.20	-0.27	3.09
	CG2DX_1C	8	-1.16	0.97	0.02	0.85
	CG2DY_1C	8	-3.57	2.88	-0.82	1.89
	IMPDX_1C	5	-0.23	0.94	0.22	0.44
	IMPDY_1C	5	-3.21	0.21	-1.71	1.40
	CG2EX_1C	8	-1.10	1.63	0.00	1.07
	CG2EY_1C	8	-3.55	2.98	-1.09	1.90
	IMPEX_1C	5	-0.22	1.75	0.66	0.89
	IMPEY_1C	5	-4.69	0.32	-1.67	1.86
	CG2FX_1C	8	-0.97	1.16	-0.13	0.83
	CG2FY_1C	8	-3.99	2.07	-1.10	1.82
	IMPFX_1C	5	-0.69	0.79	-0.00	0.53
	IMPFY_1C	5	-3.78	-0.60	-1.85	1.30
	AGE_1D	3	4.33	5.49	4.72	0.66
	CG2AX_1D	3	-4.49	0.55	-1.32	2.76
	CG2AY_1D	3	-0.33	5.62	1.77	3.34
	IMPAX_1D	2	-0.52	7.67	3.58	5.79
	IMPAY_1D	2	-4.59	-3.27	-3.93	0.93
	CG2BX_1D	3	-3.47	-0.14	-1.65	1.69
	CG2BY_1D	3	-3.05	3.97	0.15	3.55

N Obs	Variable	N	Minimum	Maximum	Mean	Std Dev
10	IMPBX_1D	2	0.91	7.77	4.34	4.85
	IMPBY_1D	2	-7.23	-3.66	-5.45	2.52
	CG2CX_1D	3	-2.73	0.18	-0.82	1.65
	CG2CY_1D	3	0.74	7.64	3.92	3.48
	IMPCX_1D	2	-0.66	6.64	2.99	5.16
	IMPCY_1D	2	0.14	3.40	1.77	2.31
	CG2DX_1D	3	-3.29	-0.38	-1.40	1.64
	CG2DY_1D	3	-1.18	4.50	1.16	2.97
	IMPDX_1D	2	-0.42	8.61	4.09	6.39
	IMPDY_1D	2	-5.44	-3.08	-4.26	1.67
	CG2EX_1D	3	-4.53	-0.07	-1.87	2.35
	CG2EY_1D	3	-1.79	3.44	0.66	2.63
	IMPEX_1D	2	1.09	7.82	4.45	4.76
	IMPEY_1D	2	-5.91	-2.86	-4.38	2.16
	CG2FX_1D	3	-3.67	0.04	-1.50	1.93
	CG2FY_1D	3	-1.36	3.25	0.42	2.48
	IMPFX_1D	2	-0.64	8.17	3.77	6.23
	IMPFY_1D	2	-5.75	-3.91	-4.83	1.30
	AGE_1E	1	5.29	5.29	5.29	.
	CG2AX_1E	1	4.18	4.18	4.18	.
	CG2AY_1E	1	-8.69	-8.69	-8.69	.
	IMPAX_1E	0	.	.	.	.
	IMPAY_1E	0	.	.	.	.
	CG2BX_1E	1	4.91	4.91	4.91	.
	CG2BY_1E	1	-9.75	-9.75	-9.75	.
	IMPBX_1E	0	.	.	.	.
	IMPBY_1E	0	.	.	.	.
	CG2CX_1E	1	0.84	0.84	0.84	.
	CG2CY_1E	1	3.26	3.26	3.26	.
	IMPCX_1E	0	.	.	.	.
	IMPCY_1E	0	.	.	.	.
	CG2DX_1E	1	5.17	5.17	5.17	.
	CG2DY_1E	1	-9.66	-9.66	-9.66	.
	IMPDX_1E	0	.	.	.	.
	IMPDY_1E	0	.	.	.	.
	CG2EX_1E	1	4.55	4.55	4.55	.
	CG2EY_1E	1	-9.77	-9.77	-9.77	.
	IMPEX_1E	0	.	.	.	.
	IMPEY_1E	0	.	.	.	.
	CG2FX_1E	1	5.12	5.12	5.12	.
	CG2FY_1E	1	-10.84	-10.84	-10.84	.
	IMPFX_1E	0	.	.	.	.
	IMPFY_1E	0	.	.	.	.
	AGE_1F	1	5.90	5.90	5.90	.
	CG2AX_1F	1	1.21	1.21	1.21	.
	CG2AY_1F	1	0.26	0.26	0.26	.
	IMPAX_1F	1	6.45	6.45	6.45	.
	IMPAY_1F	1	-5.76	-5.76	-5.76	.
	CG2BX_1F	1	0.87	0.87	0.87	.
	CG2BY_1F	1	-0.22	-0.22	-0.22	.
	IMPBX_1F	1	7.72	7.72	7.72	.
	IMPBY_1F	1	-6.23	-6.23	-6.23	.
	CG2CX_1F	1	3.66	3.66	3.66	.
	CG2CY_1F	1	11.69	11.69	11.69	.
	IMPCX_1F	1	9.55	9.55	9.55	.

N Obs	Variable	N	Minimum	Maximum	Mean	Std Dev
10	IMPCY_1F	1	5.62	5.62	5.62	.
	CG2DX_1F	1	0.90	0.90	0.90	.
	CG2DY_1F	1	-0.09	-0.09	-0.09	.
	IMPDX_1F	1	7.68	7.68	7.68	.
	IMPDY_1F	1	-6.16	-6.16	-6.16	.
	CG2EX_1F	1	0.51	0.51	0.51	.
	CG2EY_1F	1	0.13	0.13	0.13	.
	IMPEX_1F	1	7.19	7.19	7.19	.
	IMPEY_1F	1	-5.82	-5.82	-5.82	.
	CG2FX_1F	1	1.43	1.43	1.43	.
	CG2FY_1F	1	-1.07	-1.07	-1.07	.
	IMPFX_1F	1	8.27	8.27	8.27	.
	IMPFY_1F	1	-7.23	-7.23	-7.23	.
	AGE_1G	0	.	.	.	.
	CG2AX_1G	0	.	.	.	.
	CG2AY_1G	0	.	.	.	.
	IMPAX_1G	0	.	.	.	.
	IMPAY_1G	0	.	.	.	.
	CG2BX_1G	0	.	.	.	.
	CG2BY_1G	0	.	.	.	.
	IMPBX_1G	0	.	.	.	.
	IMPBY_1G	0	.	.	.	.
	CG2CX_1G	0	.	.	.	.
	CG2CY_1G	0	.	.	.	.
	IMPCX_1G	0	.	.	.	.
	IMPCY_1G	0	.	.	.	.
	CG2DX_1G	0	.	.	.	.
	CG2DY_1G	0	.	.	.	.
	IMPDX_1G	0	.	.	.	.
	IMPDY_1G	0	.	.	.	.
	CG2EX_1G	0	.	.	.	.
	CG2EY_1G	0	.	.	.	.
	IMPEX_1G	0	.	.	.	.
	IMPEY_1G	0	.	.	.	.
	CG2FX_1G	0	.	.	.	.
	CG2FY_1G	0	.	.	.	.
	IMPFX_1G	0	.	.	.	.
	IMPFY_1G	0	.	.	.	.

CG: crista galli
IMP: gravity center of maxillary implants
X: horizontal measurements
y: vertical measurements
A: reference line #6 (see Figure 7)
B: reference line #4 (see Figure 7)
C: reference line #1 (see Figure 7)
D: reference line #2 (see Figure 7)
E: reference line #5 (see Figure 7)
F: reference line #3 (see Figure 7)